Energy Conversion and Management 270 (2022) 116260

Contents lists available at ScienceDirect

Energy Conversion and Management

journal homepage: www.elsevier.com/locate/enconman

A comprehensive comparative study on the energy application of chars produced from different biomass feedstocks via hydrothermal conversion, pyrolysis, and torrefaction

Fatih Güleç [a,*], Orla Williams [a], Emily T. Kostas [b], Abby Samson [c], Edward Lester [a]

[a] Advanced Materials Research Group, Faculty of Engineering, University of Nottingham, Nottingham NG7 2RD, UK
[b] Advanced Centre of Biochemical Engineering, Bernard Katz Building, University College London, Gower Street, London WC1H 6BT, UK
[c] Department of Mechanical Engineering, University of Sheffield, Sheffield S3 7RD, UK

ARTICLE INFO

Keywords:
Char formation
Hydrothermal treatment
Pyrolysis
Torrefaction
Energy application
Biomass

ABSTRACT

Understanding the suitability of different conversion technologies for different types of biomass feedstocks is crucial in delivering the full valorisation of different types of biomasses. This is novel research which presents an extensive comparative study on how three different thermal conversion technologies (torrefaction, pyrolysis, and semi-continuous hydrothermal conversion) and process interdependencies are influenced by different feedstocks (Rapeseed (RS), Whitewood (WW), Seaweed *Laminaria digitata (LD)*)) for the optimisation of char (hydrochar/biochar) formation and their associated bioenergy applications. A wide range of processing conditions was analysed to optimise char formation and potential applications of these chars in energy production were extensively investigated. Based on the evaluation of char structures, hydrothermal conversion could be an applicable method for char production from WW and RS. The char yield of WW is in the range of 30–50 wt% at the early stage of hydrothermal carbonisation (HTC, 235 °C). Increasing temperature (>265 °C) decreased char yield but produced a higher HHV char (~30 kJ/g). Approximately 90 wt% of LD dissolved into the water at low temperatures (<200 °C) during hydrothermal conversion, leaving small amounts of char with a significant ash content (~50 wt%). During pyrolysis, RS and WW gradually decomposed and produced char with yield of ~ 35–40 wt% at 400 °C consisting of a high lignin content with a HHV of > 34 kJ/g. Similarly, LD decomposed gradually with a char yield of 45 wt% at 400 °C, but with a low HHV (~15 kJ/g) and high ash content (20 wt%). WW had relatively high char yield of ~ 60 wt% during pyrolysis at 250 °C, with a HHV of 25 kJ/g. Although RS had a high char yield (~75 wt%) with a high HHV (>30 kJ/g), the chars still contained a significant amount of volatiles. The WW char from these three thermal conversion technologies, and RS chars produced by pyrolysis and hydrothermal conversion, could have a potential application in bioenergy production. However, the ash content and low HHV make LD unsuitable for bioenergy applications.

1. Introduction

Biomass is integral to the global carbon cycle [1–3] and can be used as a clean, environmentally friendly, and inexpensive source for energy and value-added chemical production [4,5]. The undeniable potential of biomass and bioenergy to replace fossil fuels in existing processes to produce heat, electricity, and fuel for transportation makes it an attractive and promising energy resource [6–9]. As such, biomass utilisation is playing a pivotal role in achieving the new EU Green Deal targets for net-zero energy. The bioenergy applications in the EU accounted for around half of the renewable energy sources in 2019 and a substantial increase in the use of biomass and demand for bioenergy is expected due to the energy and climate change strategies [6]. The European bioeconomy is now worth over €621 billion in added value benefits, representing 4.2 % of EU GDP and employing 18 million people [10]. In order to convert biomass feedstocks into clean energy and value-added chemicals, three main biomass processing technologies such as biological conversion [11,12], thermal conversion [13–25], and physical conversion [26–28] have been identified. In general, biofuels (solid, liquid, and gas) are produced through the thermal conversion of biomass feedstocks by utilising technologies [29] such as hydrothermal conversion (carbonisation for hydrochar, liquefaction for value-added

* Corresponding author.
E-mail addresses: Fatih.Gulec1@nottingham.ac.uk, Gulec.Fatih@outlook.com (F. Güleç).

https://doi.org/10.1016/j.enconman.2022.116260
Received 9 July 2022; Received in revised form 14 September 2022; Accepted 17 September 2022
Available online 29 September 2022

chemicals, and gasification for syngas) [20,30,31], pyrolysis (slow, fast, and flash for biochar, gas and oils) [15–17,32,33], and gasification (for syngas) [18,19]. Biomass feedstocks must be utilised sustainably and efficiently to prevent deforestation and other detrimental effects on ecosystems such as loss of biodiversity/habitats [34].

There are, however, many obstacles still exist in the commercialisation of bioenergy and bioproducts via these technologies[35]. These include sourcing of biomass, differences in physical, chemical, and biological structures, a lack of cost-competitive bioproducts, ineffective biomass refinery technologies, scalability limitations of these technologies, and a limited and/or unstable supply of biofuels and bioproducts [36–38]. The chemical and biological variations in different types of biomass feedstocks can result in significant changes in their characteristics; including biomass handling (sizing, storage, feeding, etc) and biochemical composition, which also influences subsequent biochar structures [35,39–41]. Understanding the suitability of different conversion technologies for different types of feedstocks is therefore crucial in delivering the full valorisation of different types of biomasses [42,43]. Optimal valorisation pathways can be identified by investigating the formation of products such as solids (hydrochar/biochar), liquids (bio-oil and biochemicals), and gases (potentially syngas) and the most efficient application technologies of these products. The European Biochar Foundation defines biochars/hydrochars as "a heterogeneous substance rich in aromatic carbon and minerals" [44]. Biochars/hydrochars are stable, homogeneous solid fuels showing high energy densities and calorific values compared to the original biomass source [45–47]. Biochars/hydrochars can be used in a wide range of applications such as energy production [14,25], water purification [35,48], soil amendment [49], CO_2 capture [50], and nanoparticles (for making composites) [51] due to their physicochemical properties [52]. The choice of processing route and biomass type affect the potential application of the produced biochars/hydrochars.

Torrefaction is a thermal conversion (or pre-treatment) technology that converts biomass feedstocks into medium-grade solid biofuels (biochars). Biochars are stable, homogeneous, have higher energy densities and calorific values compared to the original biomass feedstock [25,45,46,53]. Torrefaction is conducted at 200–300 °C under low-oxygen or inert atmospheres and removes moisture and low energy volatiles [45,54–56]. The cost of biomass torrefaction process (drying and torrefaction) could be minimised by using the energy released via the volatiles. The volatiles released from the decomposition of hemicellulose fraction during torrefaction could be combusted to produce energy that could, in turn, minimise energy costs. Pyrolysis is another commonly used thermal conversion technology where the biomass feedstocks can be effectively converted into more valuable gas, liquid (bio-oil) and solid (biochar) products [57–59]. The chemical bonds in hemicellulose, cellulose, and lignin structures of biomass are thermally degraded in an oxygen-free environment [17,38]. Pyrolysis can be achieved in different ways 1) slow pyrolysis; 2) fast pyrolysis; and 3) flash pyrolysis, based on processing conditions [38]. Flash pyrolysis, with high temperatures (ca. 650–1000 °C), higher heating rates and short residence times (<1 s) maximises the gas yield. Fast pyrolysis, at intermediate temperatures (ca. 425–600 °C) with higher heating rates (ca. 1000–10000 °C/s) and short residence times (<3 s), increases the liquid yield [60]. For maximum biochar yield, slow pyrolysis uses lower temperatures (ca. 400 °C) with a slow heating rate and long residence times (hours to days) are required [60]. Hydrothermal conversion is an alternative promising thermal conversion technology, which uses the high inherent moisture of biomass to its advantage [61]. Hydrothermal conversion facilitates the physio-chemical transformation of biomass feedstocks in hot-compressed water to produce hydrochar, biocrude, and/or syngas, as well as value-added chemicals (ethanol, acetone, acetic acid etc.) [4]. This makes hydrothermal conversion technology a potentially viable, scalable, and energy-efficient thermo-chemical route for biomass conversion [62]. Hydrothermal conversion is usually carried out in the following states: supercritical (hydrothermal gasification, HTG, 374–550 °C and 221 bar), sub-critical (hydrothermal liquefaction, HTL, ~250–370 °C, 50–220 bar), and hydrothermal carbonisation (HTC, 180–250 °C, 15–40 bar) [18,25,63–67]. Most hydrothermal studies use batch processing, but recent developments have developed semi-continuous systems which have the potential to be scaled up for commercial use [20,25].

Comparative studies of pyrolysis, torrefaction and hydrothermal tend to focus on one material, such as olive tree prunings [68], *Miscanthus giganteus* [69], straw [70,71], or mushroom compost waste [72–74]. There are numerous studies which explore pyrolysis and hydrothermal processing [75], torrefaction and hydrothermal processing [31,76–80], and pyrolysis and torrefaction [81,82] but, again, these tend to focus on single biomass feedstocks and there are no comparative seaweed-based studies of all three thermal treatments, despite numerous individual studies [83]. Studies indicate that the preferred processing route varies with feedstock, thus comparing studies is difficult due to variations in equipment, processing conditions and limiting studies to single feedstocks or single types of feedstocks. There have very few studies which use multiple feedstocks with multiple thermal treatments. The influence of these 3 techniques on biochars produced from lignocellulosic and agricultural residues used to improve soil aggregate stability found that only hydrophobic hydrothermally carbonised chars improved aggregate stability [84]. This study did not explore the optimisation of any of the techniques and how operational parameters influence the biochar product. Furthermore, to date, no studies have compared lignocellulosic, agricultural residues and seaweeds using numerous thermal treatments.

This study is the first comparative research on how the optimal holistic biomass processing pathways and process interdependencies are influenced by feedstocks for the optimisation of char formation and the bioenergy application of the produced chars. This is also one of the first comparative studies to analyse semi-continuous hydrothermal processing in comparison to pyrolysis and torrefaction for any biomass feedstocks. The chars produced by hydrothermal conversion is defined as "hydrochar" and by pyrolysis and torrefaction are defined as "biochar" throughout the manuscript. The suitability of three different biomass feedstocks (Whitewood, Rapeseed, and Seaweed (*L. digitata)*) were therefore investigated for hydrochar/biochar formation, using three commonly used thermal conversion technologies; torrefaction, pyrolysis, and hydrothermal conversion (subcritical conditions; hydrolysis, carbonisation, and liquefaction) under a wide range of processing conditions. In this study, the optimisation of char formation is presented in detail with an evaluation of the suitability of energy application of the char products based on thermal characteristics. Additionally, the 'displacement' term, which was previously identified as a 'fingerprinting' technique for the biochars [85], has been used to make a direct comparison of three thermal conversion technologies for different type of biomass feedstocks for the first time.

2. Materials and methods

Three different biomass feedstocks were used in this study; Rapeseed residues (RS, source of agricultural waste, supplied by the University of Nottingham from Dr David Gray, Dr Filippo Bramante, and Dr Vincenzo Di Bari), Whitewood (WW, made from sawdust residues from Northern Ireland, supplied by Wolseley), and *Laminaria digitata* (LD, UK sourced brown seaweed). These feedstocks were selected as they are all domestically produced in the UK and are from three distinct types of biomasses, namely wood (WW), agricultural residues (RS) and macroalgae (LD) [5,39,86]. The rapeseed residue was obtained by the modified method presented in Ref. [87,88]. 100 g oilseed rape seeds, variety Compass, were soaked for 16 h at 4 °C, in pre-chilled sodium bicarbonate 0.1 M, pH 9.5 (extraction buffer). The soaking medium was then discarded and replaced with fresh extraction buffer. Seeds were blended with a Kenwood kMix, type BLX75, for 60 s at 400 W power (machine half power), in the extraction buffer at seed/buffer ratio 1:7 (based on

the initial seed weight), and the mix was filtered through tree layers of cheesecloth to separate the solid debris from the filtrate. The seaweed was collected at low spring tides in May 2015 near Downderry in Cornwall and prepared by following the methods outlined in the Ref [86].

2.1. Feedstocks and char characterisation

The biomass feedstocks (RS, WW, LD) were firstly ground using a Wiley Laboratory Mill (having three blades) and sieved to different particle sizes (<106 μm, 106–212 μm, 212–300 μm, 300–425 μm, 425–600 μm) in a sieve shaker for 15 min according to EN ISO 17827–2:2016, using sieves with apertures of 3,15 mm and below [89,90]. The most suitable particle sizes were used in each thermal conversion technology (specified in Section 2.2 Thermal conversion of biomass feedstocks) in order to eliminate blockages. The impact of particle size in these processes was neglected due to the narrow size distribution of the particles.

Proximate analysis: Proximate analysis was performed in a TA-Q500. Approximately 15–25 mg of sample was loaded in a platinum pan, then heated from ambient temperature to 900 °C with a heating rate of 5 °C/min with a N_2 flow rate of 100 ml/min, then held isothermally for 5 min. The N_2 flow was then replaced by air with a flow rate of 100 ml/min at 900 °C for a further 10 min [85]. The mass loss below 110 °C was considered as moisture content. The mass loss between 110 °C and 900 °C was defined as volatile matters (VM) and the loss at 900 °C under airflow was defined as fixed carbon (FC) the remaining mass after oxidation at 900 °C was defined as ash [5,91]. The proximate analysis was triplicated to eliminate the experimental error.

Ultimate analysis: The elemental compositions (carbon (C), hydrogen (H), nitrogen (N)) of biomass feedstocks and chars were determined using LECO CHN 628. Oxygen (O) content was calculated by difference [92,93]. The elemental analyses were repeated three times to reduce any systematic error. The higher heating value (HHV) of raw biomass was measured by bomb calorimeter (IKA LABORTECHNIK C4000 control) according to BS1016 (Part-5) in triplicate (results presented on dry basis). Benzoic Acid was used as the standard. However, due to the limited availability of char material, the HHV for the char samples was determined using previously defined HHV correlations and experimental CHN data. The most suitable HHV correlation for each biomass type was identified with the lowest standard deviations between the experimental and predicted HHV (Table 1, Eqs. (1)–(3)) among eleven different HHV correlations (Table S1 in Supplementary).

Density measurements: The true density (skeletal density) of biomass samples was measured by a Micromeritics AccuPyc II 1340 Gas Pycnometer. Approximately 250–500 mg sample was placed into 1.0 ml sample cell, then purged 15 times with Helium as the displacement gas. The true density was then calculated by the ratio of sample mass and sample volume of the average 20 analysis cycles [92,93]. In order to measure the tap density of biomass feedstocks, approximately 10–15 g samples were placed in a graduated cylinder (volume of 150 ml) and mechanically tap in a Copley Scientific JV 1000 tap density machine for 10 mins.

Table 1
The HHV correlations provided the lowest standard deviation for different biomass feedstocks.

Biomass Feedstocks	Correlations for Higher Heating Value (HHV)	Ref.	HHV_{Ex} (kj/g)	HHV_{Pr} (kj/g)	STDEV (±)	Eq.
Rapeseed	$HHV = 0.2949C + 0.8250H$	[94]	25.56	25.81	±0.17	(1)
Whitewood	$HHV = -3.440 + 0.517(C + N) - 0.433(H + N)$	[95]	18.94	19.64	± 0.49	(2)
L. digitata	$HHV = 0.4373C - 1.6701$	[96]	11.73	11.74	± 0.01	(3)

HHV_{Ex} and HHV_{Pr} represent the HHV measured experimentally and predicted by the correlations, respectively.

2.2. Thermal conversion of biomass feedstocks

Hydrothermal conversion: Hydrothermal conversion of the biomass feedstocks (LD, RS, and WW) was investigated in a semi-continuous rig shown in Fig. 1a [20]. A preloaded biomass sample (~5.0 g) was placed inside a 100-μm stainless steel 316L mesh, which acting as a filter at the bottom and top of the reactor, within the semi-continuous reactor. A feed stream of distilled water was pumped via a high-pressure Gilson HPLC pump and preheated to the desired temperature using a Watlow cartridge heater. The preheated water stream flows into the reactor from the bottom (up-flow), where the reaction starts with the effects of matter and energy transfer [20]. The enriched stream leaves the reactor and passes through a 100 μm filter that retains any solids that could potentially have flowed out the top of the reactor. After the filter, the process water is cooled in a heat exchanger with a stream of fresh water at room temperature. Finally, the liquid products go through a back-pressure regulator (BPR) which pressurizes the whole system, and the outflow is collected after the BPR.

The hydrothermal conversion of RS, LD and WW were investigated for a range of temperatures (100, 200, 300 °C) and pressures (4, 55, 180, 240 bar or 60, 800, 2600, and 3500 psi, respectively) (Fig. 1b) to establish the optimal conditions for hydrochar (or biomass residues depending on the process condition) production. Approximately 5.0 g of each biomass feedstock (having a particle size of 425–600 μm for RS and WW, 212–300 μm for LD) was placed between two layers of sieve mesh (100 μm) in the 316L stainless steel reactor. The hydrothermal rig was pressurised using a downflow of 20 ml/min of distilled water. The heat exchanger temperatures for up-flow were then set to the target temperature. Once the system had established the desired conditions, the up flow was then introduced to the reactor with a flow rate of 20 ml/min. The liquid product stream was cooled to about 20–30 °C in a water-cooled heat exchanger, which was collected and then stored in a freezer at −18 °C for further analysis. The hydrochars were collected from the reactor and dried in an oven at 100 °C for overnight. The chars produced by hydrothermal conversion were defined as “hydrochar” throughout the manuscript.

Pyrolysis: The pyrolysis experiments were investigated in a micro-activity test unit, illustrated in Fig. 2a. The rig consisted of a Pyrex glass tubular reactor with an internal diameter of 1.9 cm and a length of 27 cm, a temperature-controlled tubular furnace, a liquid product receiver and a gas sampling bag. The reactor was placed within a cylindrical furnace. The temperature was controlled by a vertically located thermocouple in contact with the quartz wool just over the biomass bed. The pyrolysis tests were investigated using the following procedure; approximately 5.0 g of biomass feedstocks (having a particle size of 600–850 μm for RS and WW, 212–300 μm for LD) were placed in a micro-activity reactor between two pieces of quartz wool. The reactor was located in the tubular furnace, which was preheated to 200 °C. The pyrolysis temperature was then increased to 300, 400 and 550 °C (±5 °C) with a heating rate of 20 °C/min and kept at this temperature for 60 min under a N_2 flow of 10 ml/min. The bio-oil products were condensed in the liquid product receiver using a water–ice bath, and the gas samples were collected in a 1.0 L gas sampling bag. The experimental error was calculated using a series of experiments carried out in triplicate.

Torrefaction: The torrefaction of biomass feedstocks (LD, RS and WW) was investigated in a horizontal tube furnace system (Fig. 2b) using the following conditions. Approximately 4.0 g of biomass feedstocks (having a particle size of 300–425 μm for RS and WW, 106–212 μm for LD) were placed in a porcelain crucible. The crucible was then placed in the middle zone of a quartz reactor, heated from ambient temperature to the torrefaction temperatures of 220, 250 and 280 °C

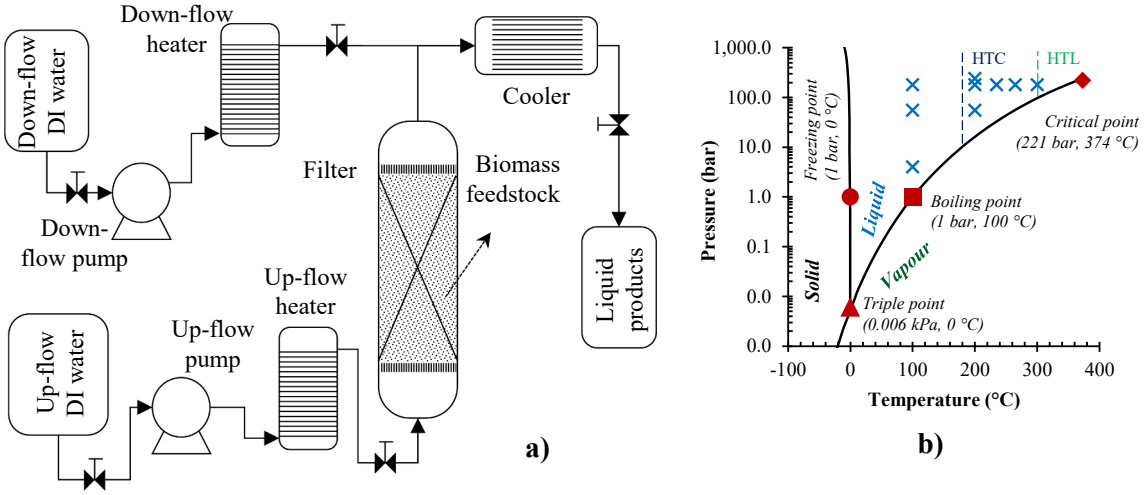

Fig. 1. a) Process flow diagram of semi-continuous hydrothermal conversion unit and b) pressure–temperature phase diagram of water [20,25,35]. Cross (x) signs represent the experiment conditions.

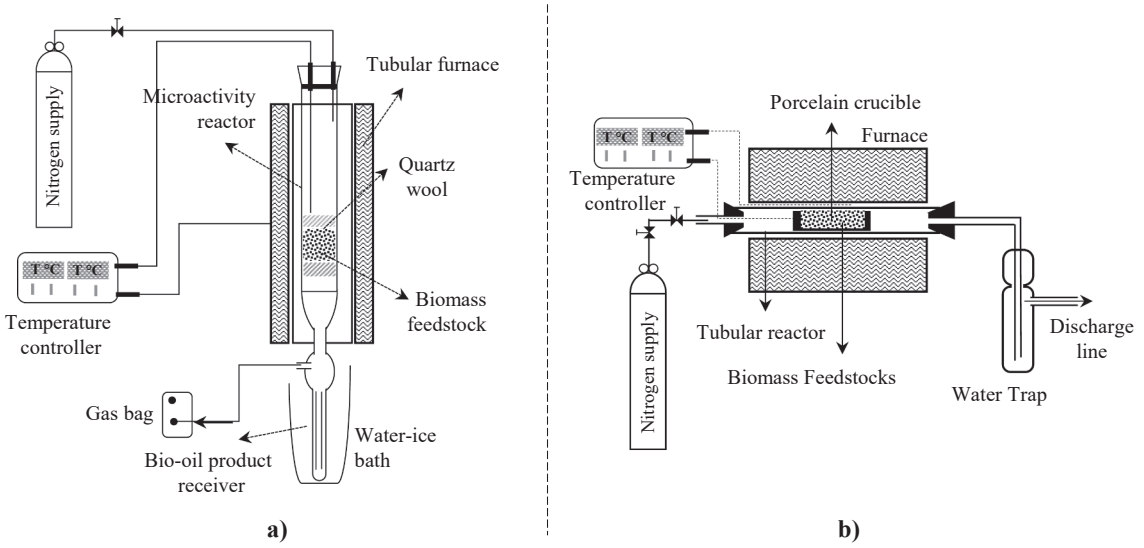

Fig. 2. Flow diagrams of a) biomass pyrolysis and b) biomass torrefaction processes [97–99].

with a heating rate of 10 °C/min under a N_2 flow rate of 1.0 L/min and the temperature was maintained at this level for 60 min. The porcelain crucible was then removed and cooled to room temperature. The experimental error was determined based on the triplicate of one set of the experiments and results were presented with error bars representing one standard deviation. The chars produced by pyrolysis and torrefaction were defined as "biochar" throughout this manuscript.

Char (hydrochar/biochar) yield of hydrothermal conversion, pyrolysis, and torrefaction was determined using (Eq. (4)) [100].

$$Char\ yield\ (C_y,\ wt.\%) = \frac{m_{Char,dry}}{m_{Biomass,dry}} * 100 \quad (4)$$

Where, $m_{Biomass,dry}$ is the dried weight of biomass (g) before thermal conversion, $m_{Char,dry}$ is the dried weight of char (g) after thermal conversion of hydrothermal treatment, pyrolysis, and torrefaction.

2.3. Thermal analysis of chars

A thermogravimetric characterisation technique was used to investigate the devolatilization behaviours of the biomass feedstocks and chars. This technique has been used to quantify components such as hemicellulose, cellulose, and lignin [85] using the thermogravimetric (TG) and differential thermogravimetric (dW/dt) curves [101]. Approximately 15–25 mg of char was loaded in a platinum pan in a TA-Q500 instrument. The sample was then heated from ambient temperature to 900 °C with a heating rate of 5.0 °C/min under N_2 flow rate of 100 ml/min and held at this temperature for about 5 min. N_2 was then replaced by air (to combust the fixed carbon) with a flow rate of 100 ml/min at 900 °C for a further 10 min [85]. In order to characterise the impact of process conditions of thermal conversion technologies on char formation and structure, the level of "displacement" was determined with the global sum of all absolute values of the differences between the original and experimental differential thermogravimetric (DTG) profiles as defined in Eq-5 [20,85].

$$Displacement = \sum_{T_s}^{T_f} \left(\left| \left(\frac{dw}{dt} \right)_{bf,T} - \left(\frac{dw}{dt} \right)_{hc,T} \right| \right) \quad (5)$$

Where, T_s and T_f are the temperatures of thermal decomposition starts and finished between (25–900 °C), $(dW/dt)_{bf,T}$ and $(dW/dt)_{ch,T}$ are the weight loss rate of biomass feedstocks and chars at the specific temperatures in the thermal decomposition process.

3. Results and discussions

3.1. Characterisation of feedstocks

The ultimate analysis, proximate analysis, densities and HHV of the biomass feedstocks are presented in Table S2 in Supplementary. The ultimate analysis shows a wide range of carbon and oxygen composition for these biomass feedstocks. WW and RS have the highest VM (~79 wt %) and lowest FC (~11–13 wt%) ratios while LD provides lower VM (~55 wt%) and higher FC of ~ 18 wt%. Furthermore, the LD has a high ash content (~18 wt%) compared to the other feedstocks, which is in agreement with previous findings [102]. LD also had much higher Tap and True densities and lower HHV compared to RS and WW. The following sections (3.3. Thermal analysis of chars) provide further information on the proximate and ultimate analysis of each type of hydrochars/biochars and the impact of thermal conversion technologies.

3.2. Thermal conversion of biomass feedstocks

The char yields of RS, WW and LD generated from the three thermal conversion technologies (hydrothermal conversion (including HTL, HTC, and HTH), pyrolysis, and torrefaction) are presented in Fig. 3. Regardless of thermal conversion technology, the increase in the operating temperature decreases the biochar/hydrochar yield, which is in agreement with previous findings [103,104]. The decrease in biochar/hydrochar yields can be attributed to the gradual thermal decomposition of biomass structure as lignocellulosic biomass begins to carbonise at temperatures above 180 °C [63,105,106] when the cellulosic and hemicellulosic polymers disintegrate into monomers/oligomers [1]. The main biomass components, hemicellulose, cellulose and lignin, gradually decompose at temperatures of 220–315 °C, 280–400 °C and 160–900 °C, respectively [17,85,107].

Hydrothermal conversion (Fig. 3a) showed temperature to have a significant effect on char yield while pressure appears to have a minimal impact on biomass solubility (presented in Fig. S1 in Supplementary materials). WW and RS produced a smaller water-soluble portion (~5–7 wt% and ~ 20 wt%, respectively) at the low hydrothermal conversion of 100–150 °C while both RS and WW demonstrate higher decomposition and carbonisation levels (with a char yield of ~ 50 wt%) at 200 °C. This could be attributed to the carbonisation temperature of lignocellulosic biomass (RS and WW), which starts above 180 °C [63,105,106] in which

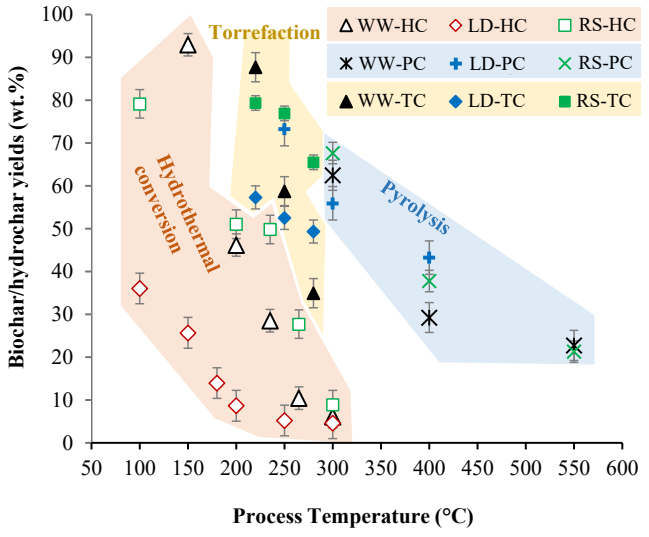

Fig. 3. Biochar/hydrochar yields of RS, WW, and LD under the thermal conversion techniques of hydrothermal conversion (HC), pyrolysis (PC), and torrefaction (TC).

the cellulosic and hemicellulosic polymers were breakdown into monomers/oligomers [1]. LD, on the other hand, demonstrated much higher water-soluble portion (~60–65 wt%) at 100–150 °C and the increase in the process temperature to 200 °C resulted in a char yield of ~ 10 wt%. This results from the differences in biochemical compositions of LD compared with RS and WW. As different biochemical structures required different decomposition temperature and behaviour under hydrothermal conversion. For example, the biopolymers in raw LD, mainly polysaccharides alginate and fucoidan, and possibly the protein fraction, significantly degrade at ~ 180–320 °C. At the hydrothermal liquefaction (HTL) condition (300 °C), all three biomass feedstocks produced ~ 5–10 wt% of hydrochar yield. Above 300 °C, the biomass feedstocks depicted low levels of char formation where the cellulosic and hemicellulosic polymers in biomass structures break into monomers which are subsequently released into the water phase. At a high temperature (>265 °C), the cellulosic structure of WW and RS were significantly degraded due to the catalytic effects of the hydroxyl (OH–) and hydronium (H +) ions [20] in hydrothermal liquefaction processes. The following section (3.3.1. Hydrochars produced by hydrothermal conversion) provides further information on the thermal decomposition of each hydrochars and the impact of hydrothermal process conditions on the formation of hydrochar structures.

The biomass feedstocks provided lower char yields via hydrothermal conversion (Fig. 3a) compared to pyrolysis (Fig. 3b). This can be attributed to high solvation rates and the catalytic properties of water in the hydrothermal conversion processes [20] leading to a large amount of the fixed carbon within the biomass being converted and lost (i.e. not remaining as a char product). These biomass feedstocks provide different biochemical structures, which are decomposed at different temperatures through pyrolysis and torrefaction processes. WW consists of hemicellulose (23–26 wt%), cellulose (48–56 wt%), and lignin (26–30 wt%) structures [108]. The thermal decomposition of hemicellulosic, cellulosic, and lignin structures are between 200 and 315 °C, 280–400 °C, and 160–900 °C, respectively, [17,85,107]. RS usually has a significant amount of extractives (19.4 wt% including proteins, lipids, waxes, resins, free sugars, gums, and tannins) in addition to hemicellulose (41.4 wt%), cellulose (28.6 wt%) and lignin (5.0 wt%) [109]. The extractives are defined as ethanol extractives (lipids, waxes, and resins – the highest part of it Triglycerides) and water extractives (free sugars, gums, and tannins) [110]. LD (seaweed) compose of carbohydrates (35–55 wt%, i.e. Mannitol 9–20 wt%, Fucose/Fucoidan 9–12 wt%, Laminarin content 13–41 %, Glucose 3–36 wt%), proteins (5–12 wt%), and minor amount of phenolic substances (phlorotannin), lipids (small amounts) and ash [111].

In the torrefaction process (Fig. 3c), WW demonstrated the highest decomposition via the torrefaction process, as char yield was ~ 87 wt% at 220 °C and decreased to ~ 35 wt% at 280 °C, which could be attributed to the thermal decomposition of hemicellulose [112] and cellulose structures. As thermal decomposition of the hemicellulosic structure in WW begins at ~ 200 °C, where the partial hydrolysis of glycosidic linkages, the decarboxylation of side chains, and the exothermic condensation of molecules occur [108]. The β-glycosidic bonds rupture at ~ 220 °C. At a temperature between 220 and 280 °C, active disintegration occurs via condensation, oxidation, and polymerization reactions [108]. However, the low biochar yield of WW (35 wt%) at 280 °C is not only attributed to the decomposition of hemicellulose but also the decomposition of cellulose due to the long residence time of torrefaction (60 min). As the thermal decomposition of the cellulosic structure of WW begins at 280 °C and ended at about 370 °C, which is in line with the literature [113], where significant thermal decomposition of cellulose was observed at 300 °C. RS and LD do not demonstrate the same level of thermal decomposition from the torrefaction process, as the char yield decreased from 79 to 65 wt% for RS, and from 57 to 49 wt % for LD, as temperature increased from 220 to 280 °C, which could be attributed to the heterogeneous structure of RS and LD. For example, the main structure of microalgae are lipids, proteins, carbohydrates which

usually decompose around 259–470 °C, 245–312 °C, and 139–397 °C [114], respectively. Char yield therefore depends on the decomposition parts of these main components under the torrefaction conditions. A detailed discussion with proof using thermal decomposition of biochars is provided in section "3.3.3. Biochar produced by torrefaction".

In pyrolysis, lower biochar yields were produced at higher pyrolysis temperatures due to increasing thermal decomposition, as higher energy is required to achieve a higher thermal decomposition of the polymeric bonds in the biomass (Fig. 3b). Despite the differences in proximate and ultimate analyses, WW and RS produced similar char yields, which is ~ 65 wt% at 300 °C, which can be attributed to the decomposition of hemicellulosic structure in WW and RS (as mentioned previously that hemicellulosic structures are decomposed at a temperature range of 200–315 °C [108]. In addition to hemicellulose, decomposition of protein and sugars also contributed to the biochar yield since proteins and sugars also endothermically decompose between 185 and 280 °C [115] and 280–300 °C [116], respectively. The biochar yield of RS and WW decreased to 29–37 wt% at 400 °C due to the further decomposition of cellulose (48–56 wt%) structure in WW and cellulose (28.6 wt%), part of extractives (mainly triglycerides) in RS. Since thermolysis of triglycerides occurs above 300 °C with cracking above 350 °C [117]. Much lower biochar yield (~21 wt%) was observed at 550 °C for WW and RS due to the complete decomposition of cellulose, hemicellulose and partial decomposition of lignin structures in WW and cellulose, hemicellulose, extractives, and partial decomposition of lignin in RS. Furthermore, LD produced high char yields via pyrolysis; 55 wt% at 300 °C and 43 wt% at 400 °C (Fig. 3b) compared to hydrothermal conversion (Fig. 3a), which could be attributed to the catalytic properties of water molecules in hydrothermal conversion decomposing seaweed structure at a lower temperature than thermal decomposition conditions. As presented in the literature, pyrolysis of microalgae, the biopolymers (alginate) are decomposed at ~ 240–260 °C, carbohydrates/sugars are decomposed at 245–312 °C, proteins are decomposed 139–397 °C, and lipids are decomposed 259–470 °C [114,116]. A detailed discussion with proof using thermal decomposition of biochars is provided in Section "3.3.2. Biochar produced by pyrolysis".

3.3. Thermal analysis of chars

3.3.1. Hydrochars produced by hydrothermal conversion

3.3.1.1. Hydrothermal conversion of Whitewood:. Fig. 4 shows the proximate and ultimate analyses of raw and hydrochars produced by the hydrothermal conversion of WW at different temperatures and pressures. Hydrolysis (150 °C at 180 bar (2600 psi)) and early-stage of carbonisation (200 °C at 55–240 bar (800–3500 psi)) conditions had an insignificant effect on the proximate and ultimate analyses of chars produced by WW compared to raw WW. However, for HTC above 235 °C, increasing process temperature increased the FC ratio while decreasing the VM in the hydrochar (Fig. 4a). Similar trends were also noted for the ultimate analysis (Fig. 4b). The hydrochars produced at above 235 °C provide higher carbon and lower oxygen ratio, which results in higher HHV of hydrochars (Fig. 4a).

Fig. 5 shows the thermal decomposition characteristics (Weight loss, Weight-loss rate, and Displacement) of raw biomass and hydrochars produced by the hydrothermal conversion of WW at different temperatures and pressures. The thermal decomposition of the hydrochar produced at 150 °C provides the main weight loss (degradation) peak with a weight loss rate of ~ 6.3 wt. %/min at ~ 338 °C. This can be attributed to the higher cellulose-lignin structures which are illustrated by a shoulder before ~ 300 °C (lower hemicellulose-cellulose) and tail after ~ 375 °C (lignin) in Fig. 5. This is identical to the profile of raw WW (Fig. 5b) [20]. The shoulder before ~ 300 °C disappeared due to degradation of the hemicellulosic structures of WW for the hydrochars produced at > 200 °C (Fig. 5b). Thus, the hydrochars produced at 200–235 °C, show a strong cellulose-lignin structure. The structural differences between hemicellulose (compared to cellulose), combined with differences in crystallinity and molecular weight, resulting in high levels of degradation of the hemicellulose under hydrothermal treatment [20]. However, the pressure used at 200 °C (55–240 bar (800–3500 psi)) appears to have an insignificant impact on the hydrochar structure (Fig. 5c and Fig. S1).

At higher temperatures (>265 °C), the cellulosic structure of WW was significantly degraded and produced a char with a strong lignin structure, most likely due to the catalytic effects of the hydroxyl (OH^-) and hydronium (H^+) ions [63,107]. The weight loss rate was approximately 5.5–7.0 wt.%/min at temperatures below 235 °C, where the hydrochars have strong cellulosic structure. Above temperatures of 265 °C, the weight loss ranged between 1.0 and 1.5 wt.%/min, and the resultant hydrochars show strong lignin signals from the TGA profile. The higher displacement results from greater decomposition of the biomass structure at the specified condition during the biomass processing technology, as it is determined by the sum of the absolute value of the differences between the DTG profiles of feedstocks and chars [20,85]. Hydrochars produced at 265–300 °C demonstrated greater

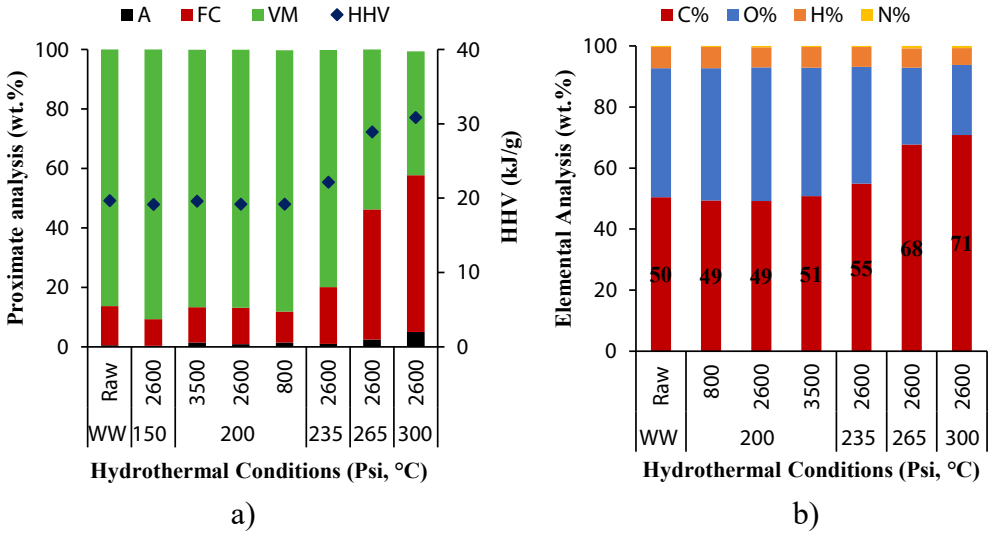

Fig. 4. a) Proximate analysis (dry basis, A: Ash, FC: Fixed carbon, VM: Volatile matter) and Higher Heating Value (HHV), b) Elemental analysis (ash free basis, C: Carbon, O: Oxygen, H: Hydrogen and N: Nitrogen) of hydrochars produced by the hydrothermal conversion of WW at different temperature and pressures.

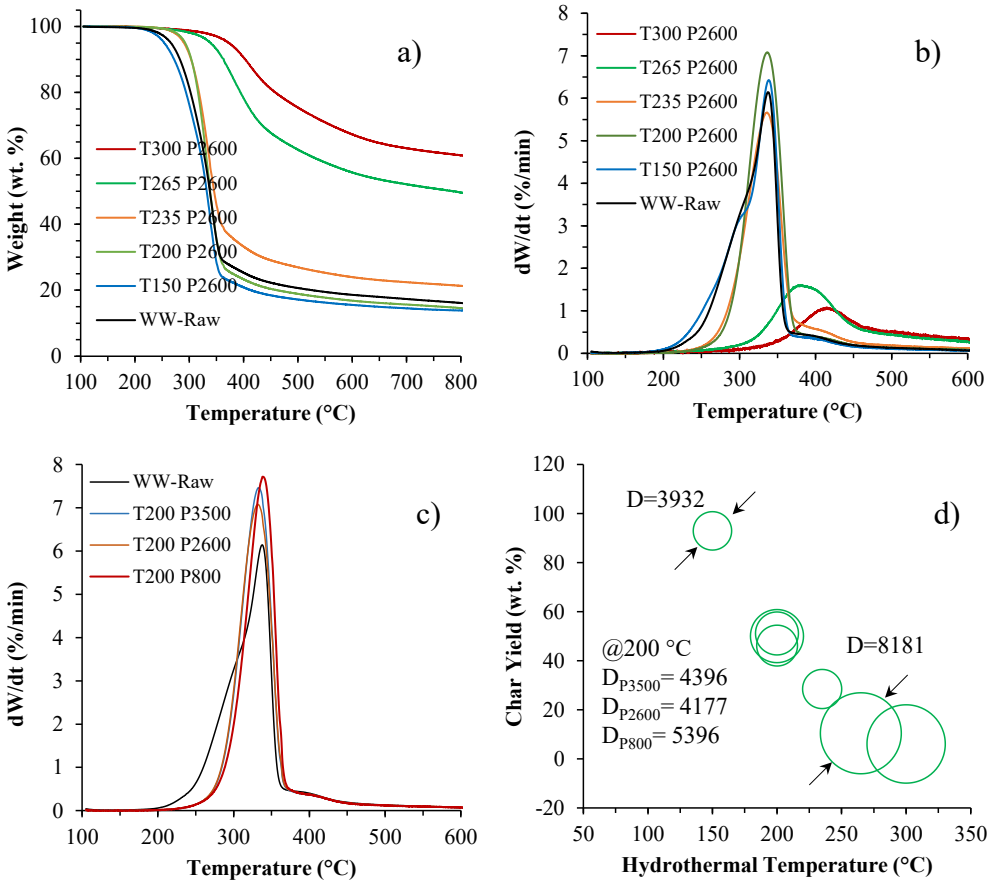

Fig. 5. a) Weight loss (wt.%), b-c) Weight-loss rates (%/min) and d) Displacement of hydrochars produced by the hydrothermal conversion of WW at different temperatures and pressures.

levels of 'displacement' at ~ 7900–8100, respectively (Fig. 5d). These higher displacement values suggest that the impact of the process conditions on the biomass is significant.

3.3.1.2. Hydrothermal conversion of Rapeseed:. Fig. 6 demonstrates the proximate and ultimate analysis of the hydrochars produced by RS at a range of hydrothermal conversion conditions. The hydrochars produced from RS at low to medium temperatures (100–265 °C) show small differences in the ratio of VM and FC. However, the ash content significantly increases from 3.7 wt% to 12–18 wt% (Fig. 6a). The increase in ash content could be attributed to the proportion of biomass structure breaking down into the water via hydrothermal conversion, while the ash remained in the final char structure. At HTL conditions of 300 °C, the FC ratio proportionally increased from ~ 12 wt% to ~ 23 wt%, while the

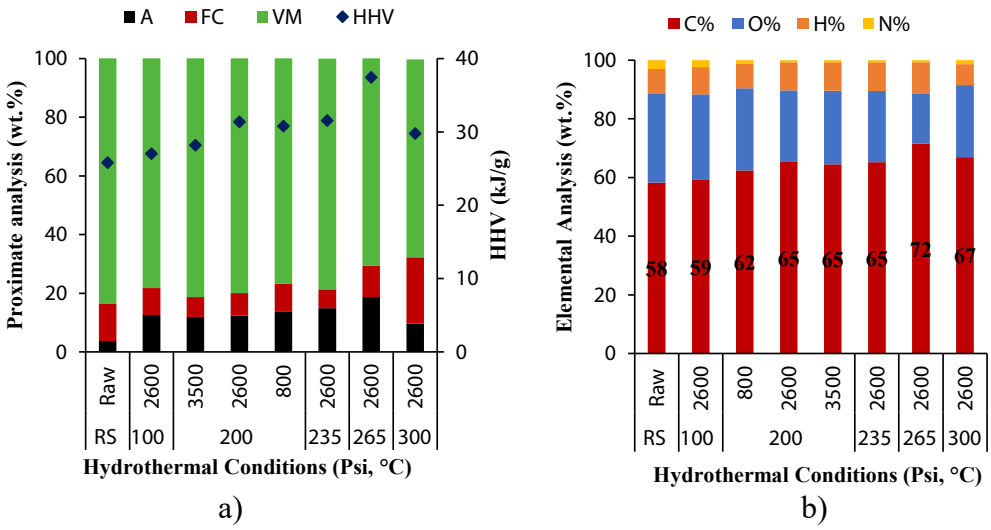

Fig. 6. A) Proximate analysis (dry basis, A: Ash, FC: Fixed carbon, VM: Volatile matters) and Higher Heating Value (HHV), b) Elemental analysis (ash-free basis, C: Carbon, O: Oxygen, H: Hydrogen and N: Nitrogen) of hydrochars produced by the hydrothermal conversion of RS at different temperature and pressures.

VM ratio decreased from ~ 84 wt% to ~ 67 wt%. Conversely, the carbon content gradually increased (from 58 wt% to 72 wt%), while the oxygen level decreased with an increase in hydrothermal conversion temperature (Fig. 6b).

Fig. 7 presents the thermal decomposition characteristics of raw and hydrochars produced by the hydrothermal conversion of RS. Raw RS depicts three main stages of thermal degradation, representing hemicellulosic-cellulosic structures (at 250–320 °C), cellulose-lignin structure (at 320–390 °C) and a lignin structure (above 390 °C) as a shoulder. The hydrochars (or biomass residues) produced at 100 °C also show three main stages of thermal degradation as demonstrated in Fig. 7b. The hemicellulosic structure was completely degraded at an HTC temperature of 200 °C, therefore, the hydrochars produced between 200 and 300 °C (HTC-HTL conditions) provides more cellulose-lignin structures. Although the lignin structure became more apparent at 300 °C as a peak (instead of the shoulder), the cellulose-lignin structure is still a big portion of the hydrochar produced at 300 °C. The insignificant structural change in RS through hydrothermal conversion was also demonstrated with low displacement at ~ 2100 at 100 °C and ~ 3500 at 300 °C (Fig. 7d). The low level of displacement indicates that the hydrochars produced by RS maintain a chemical structure similar to the feedstock despite the significant decrease in the hydrochar yield (demonstrated previously in Fig. 3a). The insignificant change in the hydrochar structures produced by RS at different conditions could be attributed to the heterogeneous contents of RS residue [118]. As major components, RS residues usually contain ~ 11 wt% of water extractives, ~8 wt% of hemicellulose, ~9 wt% of cellulose, ~4 wt % of lignin, ~34 wt% of ethanol extractives, and ~ 30 wt% of crude protein [110].

3.3.1.3. Hydrothermal conversion of L. digitata:. The proximate and ultimate analyses of hydrochars produced by the hydrothermal conversion of LD are presented in Fig. 8. As previously demonstrated in Fig. 3, LD contained a significant amount of a water-soluble portion (~60–65 wt %) at the hydrolysis conditions of 100–150 °C, 2600 psi. LD had generated significantly lower char yields, compared to WW and RS, under the same processing conditions. The increase in the hydrothermal conversion temperature significantly increased the ash content from 8.1 wt% to 66 wt%, while FC and VM contents significantly decreased from 32 wt% to 21 wt% and 60 wt% to 12 wt%, respectively (Fig. 8a). The ultimate analysis of hydrochars (ash-free basis, Fig. 8b) demonstrates that the carbon content gradually increased while the oxygen content decreased with increasing HTC temperature. Although the increase in the carbon content slightly enhanced the HHV of hydrochars, the hydrochars have a low HHV of 16–18 kJ/g, which decrease the potential application of these chars in energy production through combustion.

Thermal decomposition of raw and hydrochars produced by the hydrothermal conversion of LD are presented in Fig. 9a-c. The biopolymers in raw LD, mainly polysaccharides alginate and fucoidan, and possibly the protein fraction, which degrade at ~ 180–320 °C, were significantly impacted by increases in hydrothermal temperature. The biopolymer peak completely disappeared at the hydrothermal conversion at 160 °C. A new degradation peak between ~ 250–370 °C appeared for hydrochars produced at HTC conditions. Fig. 9c indicates that the lower pressure of HTC (at 200 °C) resulted a significant shift in the thermal decomposition of biopolymers and the peak temperature was shifted from 295 °C (240 bar (3500 psi)) to 344 °C (55 bar (800 psi)). The displacement level of LD was ~ 3400 at 100 °C (Fig. 9d), which is higher than RS (~2100) under the same conditions. Furthermore, the displacement level of hydrochars increased to ~ 7300 at

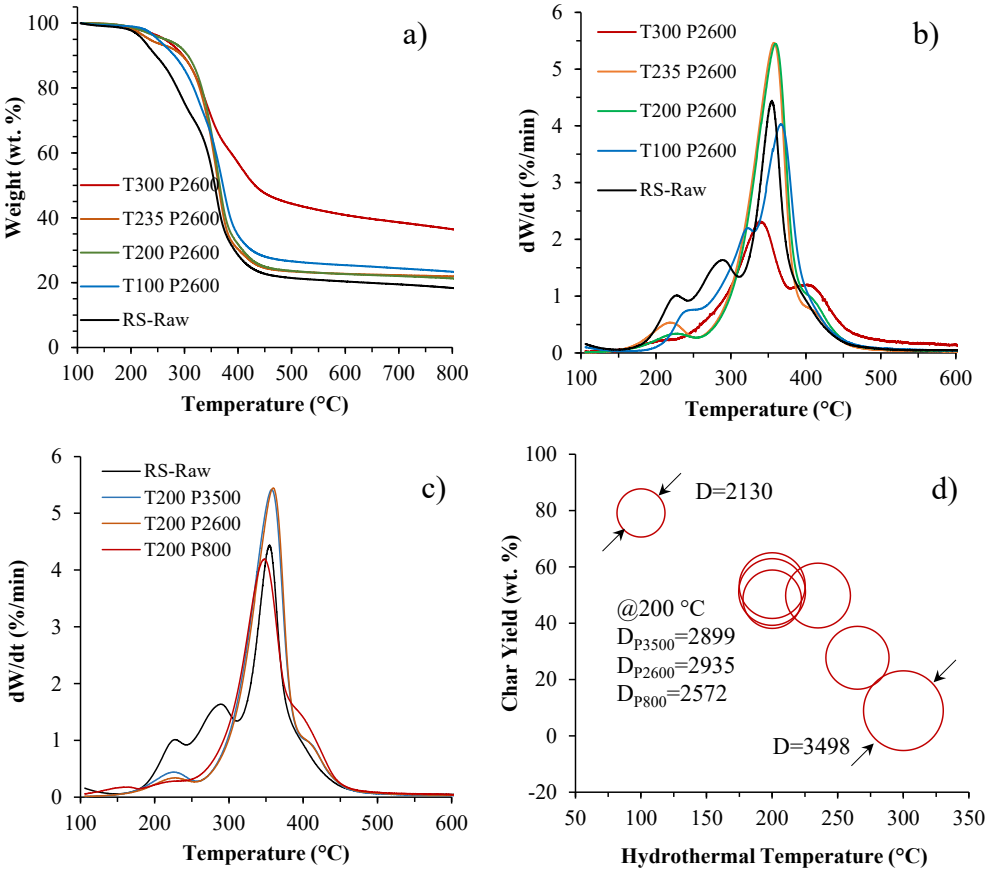

Fig. 7. A) Weight loss (wt.%), b-c) Weight-loss rates (%/min) and d) Displacement of hydrochars produced by the hydrothermal conversion of RS at different temperatures and pressures.

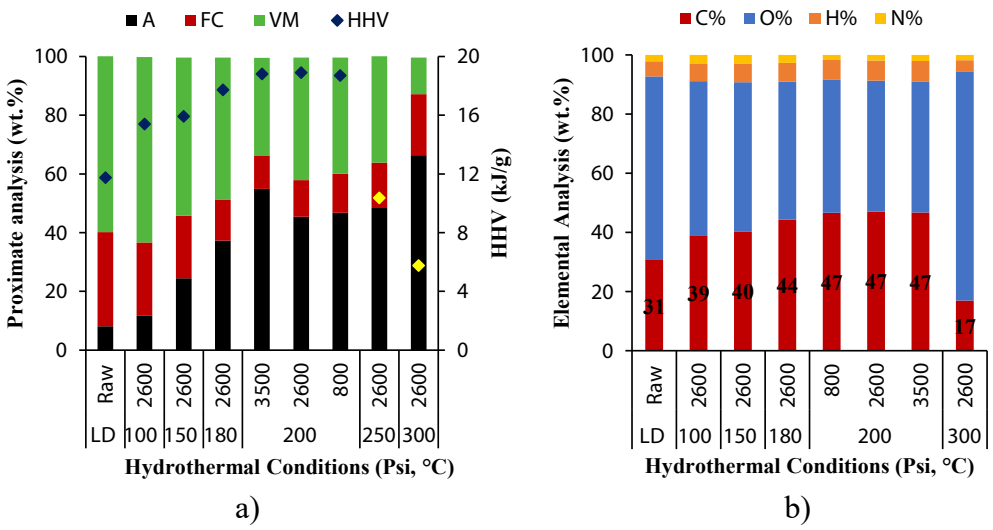

Fig. 8. a) Proximate analysis (dry basis, A: Ash, FC: Fixed carbon, VM: Volatile matters) and Higher Heating Value (HHV), b) Elemental analysis (ash-free basis, C: Carbon, O: Oxygen, H: Hydrogen and N: Nitrogen) of hydrochars produced by the hydrothermal conversion of LD.

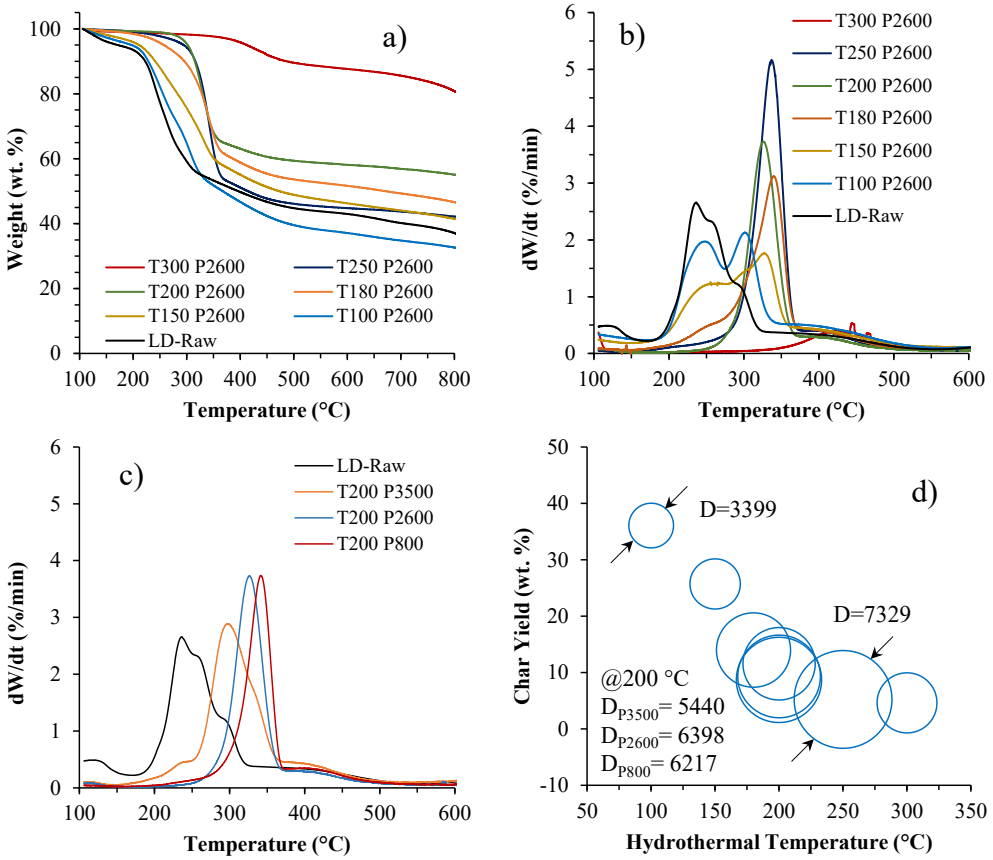

Fig. 9. a) Weight loss (wt.%), b-c) Weight-loss rates (%/min) and d) Displacement of hydrochars produced by the hydrothermal conversion of LD at different temperatures and pressures.

250 °C. However, displacement at liquefaction conditions (300 °C) of ~ 4500 could be attributed to the low char yield and high ash content. In general, the significant ash content and low HHV of the LD hydrochars would make them unsuitable for energy generation processes.

3.3.2. *Biochar produced by pyrolysis*

The proximate and ultimate analyses of biochars produced by the pyrolysis of these three different biomass feedstocks (RS, WW, and LD) are presented in Fig. 10. Predictably, increasing pyrolysis temperature gradually increased the FC content of biochar while decreasing the VM ratio (Fig. 10a). At the highest pyrolysis temperatures (400 °C for LD, and 550 °C for RS and WW), the FC ratios increased to 64 wt% for LD, and to 66 wt% and 84 wt% for RS and WW, respectively. Similarly, the ash content of the produced biochars increased to a higher proportion with increasing pyrolysis temperature. However, the increase in ash for WW was lower than that of RS and LD. Furthermore, the ash content of

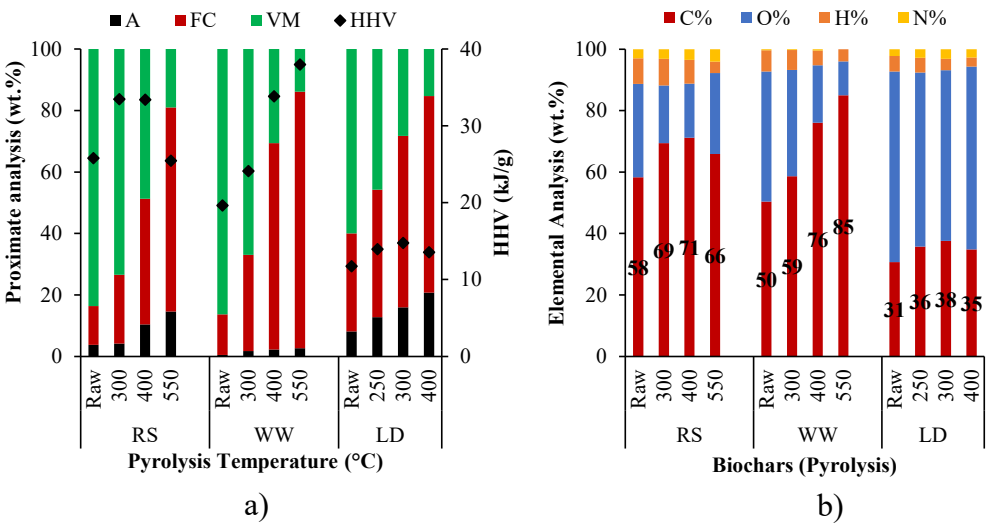

Fig. 10. a) Proximate analysis (dry basis, A: Ash, FC: Fixed carbon, VM: Volatile matter) and Higher Heating Value (HHV), b) Elemental analysis (ash free basis C: Carbon, O: Oxygen, H: Hydrogen and N: Nitrogen) of biochars produced by pyrolysis of RS, WW, and LD.

LD biochars produced by pyrolysis (Fig. 10a) is lower (13–21 wt% at 250–400 °C) than the ash content of LD hydrochars (45–66 wt% at 200–300 °C) produced by HTC and HTL (Fig. 8a), which could be attributed to the proportion of ash (proximate analysis). As demonstrated in Section 3.2, the hydrochar yield of LD is<10 wt% at HTC and HTL conditions. Since the hydrothermal conversion (HTC and HTL) mainly decomposes/liquefies the organic compounds in the biomass feedstocks, the char also has a higher ash content. Although some of the ash can be flow out of the reactor via water, this study shows that most remains in the hydrochar. Similarly, pyrolysis of LD provides a higher char yield partially due to the lower ash content in the final biochar products, as compared to hydrothermal conversion. WW biochars provided the highest increase in HHV (from 19.6 to 38.0 kJ/g), which followed by RS (25.8 to 33.5 kJ/g). WW showed an increase in carbon content from elemental analysis (with a minimum oxygen content level) with an increase in pyrolysis temperature (from 50 to 85 wt%), while the

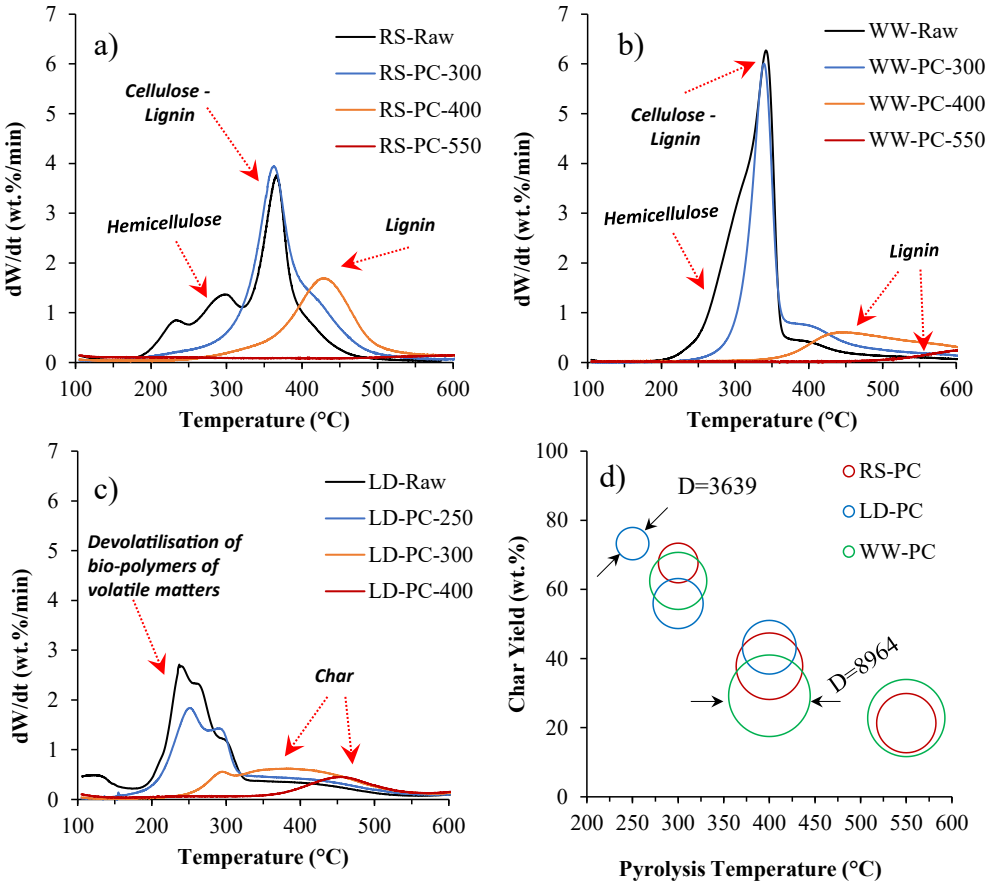

Fig. 11. a) Weight-loss rates (%/min) of biochars produced by pyrolysis of a) RS, b) WW, and c) LD at different temperatures and d) Displacement of these biochars.

carbon content of RS and LD was slightly enhanced via pyrolysis temperatures (from 58 to 71 wt% and 31 to 38 wt% respectively).

Further understanding of the differences between proximate and ultimate analysis can be gained via the thermal decomposition of biochars in Fig. 11. The chemical bonds in hemicellulose, cellulose and lignin structures of biomass feedstocks gradually degrade with increasing temperature [20]. WW biochars produced via pyrolysis exhibit a gradual decomposition, where the hemicellulose was completely removed from the biochar at 300 °C (Fig. 11b). The WW biochars produced at temperatures higher than 400 °C have solely lignin structures (Fig. 11b), which is similar to the WW hydrochars produced by HC (Fig. 5b). However, the thermal decomposition trends of RS and LD biochars produced via pyrolysis (Fig. 11a and Fig. 11c) demonstrate significant differences between the equivalent hydrochars produced via hydrothermal conversion (Fig. 7b and Fig. 9b). The RS biochars show a gradual decomposition, with the hemicellulose-cellulose composition disappearing at 300 °C, cellulose-lignin composition disappearing at 400 °C, and the lignin composition partially removed at 550 °C. Similarly, biopolymers in LD gradually decomposed by pyrolysis temperatures and only char structure appeared at the pyrolysis temperature above 300 °C (Fig. 11c). Fig. 11d shows the displacement level of the biomass feedstocks under pyrolysis conditions. The char yield decreased as the displacement level increased with an increase in the pyrolysis temperature. The highest displacement level reached at 400 °C for all these biomass feedstocks; was ~ 8900 for WW, ~7300 for RS, and ~ 5900 for LD. The displacement level decreased for RS and WW at 550 °C. 400 °C appears to be the optimised pyrolysis temperature for RS and WW, as the pyrolysis process has the highest impact on biochar production with a reasonable yield.

3.3.3. *Biochar produced by torrefaction*

The ultimate and proximate results for biochars produced by torrefaction are presented in Fig. 12. WW demonstrates the highest enhancement via the torrefaction process, as the FC ratio increases from ~ 17 wt% at 220 °C to ~ 54 wt% at 280 °C. This is likely due to strong hemicellulosic-cellulosic structures present in WW (Fig. 12a). As the gradual thermal decomposition of lignocellulosic biomass structure begins at temperatures > 180 °C [63,105,106] when the cellulosic and hemicellulosic polymers disintegrate into monomers/oligomers [1]. During the torrefaction, the main biomass components, hemicellulose, cellulose and lignin, gradually decompose at temperatures of 220–315 °C, 280–400 °C and 160–900 °C, respectively [17,85,107]. Although the FC ratio of LD biochar was significantly improved during low-temperature torrefaction (~32 to ~ 54 at 220 °C), further temperature increases did not significantly increase the FC ratio. Similarly, RS did not show a high level of thermal decomposition via the torrefaction process, as the FC only increased slightly from ~ 14 to ~ 20 wt% with a temperature increase from 220 to 280 °C (Fig. 12a). The carbon content of WW and RS was enhanced by torrefaction (~22 wt% for WW, ~12 wt% for RS), but only increased by approximately 7 wt% for LD (Fig. 12b). Carbon contents are similar to the chars produced during pyrolysis (Fig. 10). The HHV of RS and WW biochars (Fig. 12a) shows improvement with increasing torrefaction temperature, but not with LD biochars.

The thermal decomposition of raw and biochars produced by torrefaction is presented in Fig. 13a-c. Similar to pyrolysis biochars, torrefaction biochars exhibited a gradual decomposition of hemicellulose, cellulose and lignin structures with increasing temperature. The hemicellulosic structure of RS was partially decomposed at 220 and 250 °C and the biochars produced at 280 °C showed significant cellulosic structures, combined with a shoulder presenting the lignin content (Fig. 13a). This degradation could be attributed to the complete decomposition of proteins at 220 °C and partial decomposition of sugars at 280 °C, since proteins and sugars also endothermically decompose between 185 and 280 °C [115] and 280–300 °C [116], respectively. However, unlike pyrolysis, the final biochar contains significant amount of triglycerides since thermolysis of triglycerides occurs above 300 °C and cracking above 350 °C [117]. As for WW, thermal decomposition of the hemicellulosic structure in WW begins at ~ 200 °C, where the partial hydrolysis of glycosidic linkages, the decarboxylation of side chains, and the exothermic condensation of molecules occur [108]. The hemicellulosic and cellulosic structures of WW completely decomposed by 250 °C and 280 °C, respectively. Biochars produced at 280 °C therefore consist of predominantly lignin structures (Fig. 13b, red line). The biopolymers in raw LD significantly decomposed at 220 °C, with shifted char peaks, as well as showing strong char structures with increasing temperature. A significant portion of LD was decomposed before 220 220 °C, which could be attributed to the decomposition of proteins, which are decomposed 139–397 °C [114,116]. At higher torrefaction temperatures 250–280 °C, a further decomposition on biopolymers (alginate), carbohydrates/sugars, lipids occurs as the biopolymers (alginate) decomposing at ~ 240–260 °C, carbohydrates/sugars are decomposed at 245–312 °C, with lipids decomposing 259–470 °C [114,116]. The displacement level of WW biochar is ~ 4000 at 220 °C

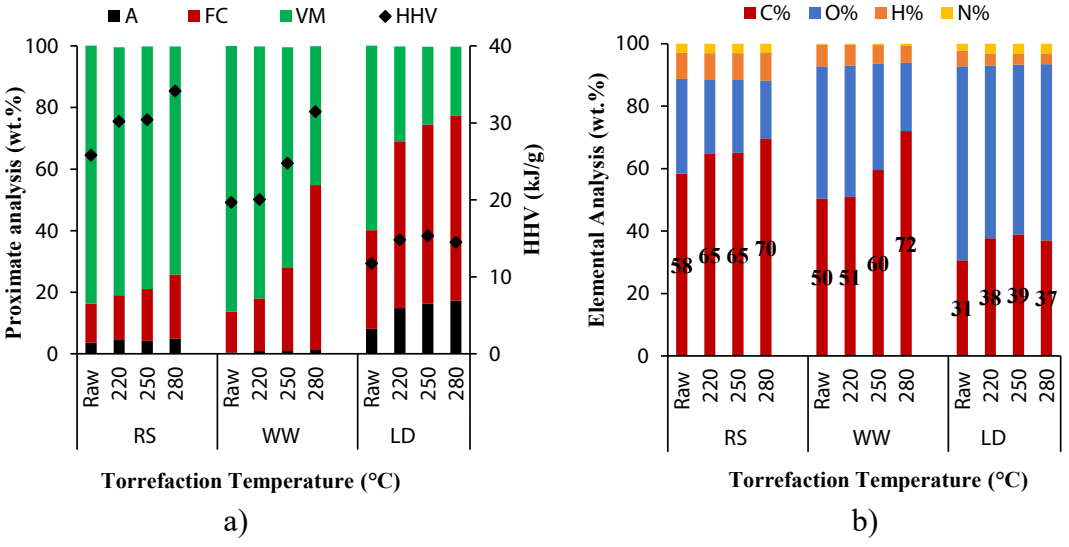

Fig. 12. a) Proximate analysis (dry basis, A: Ash, FC: Fixed carbon, VM: Volatile matter) and Higher Heating Value (HHV), b) Elemental analysis (ash free basis C: Carbon, O: Oxygen, H: Hydrogen and N: Nitrogen) of biochars produced by torrefaction of RS, WW, and LD.

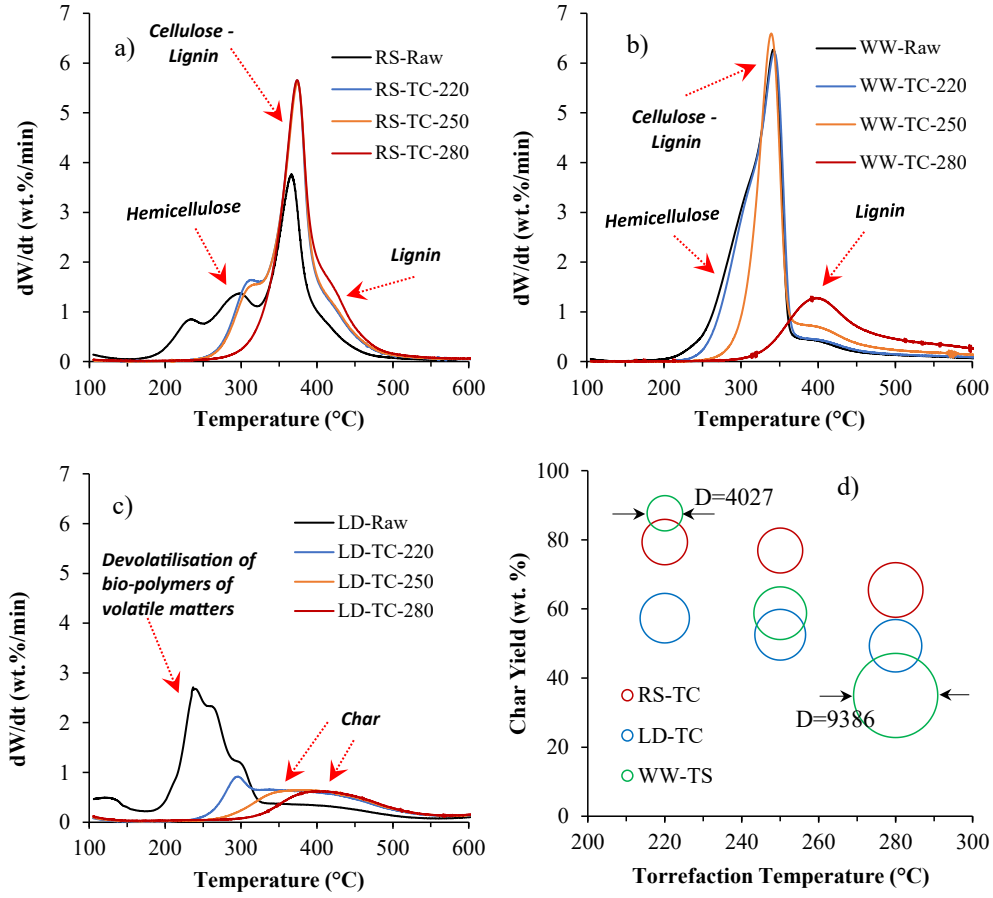

Fig. 13. a) Weight-loss rates (%/min) of biochars produced by torrefaction of a) RS, b) WW, and c) LD at different temperatures and d) Displacement of these biochars.

increasing significantly to ~ 9400 at 280 °C. However, the increase in the displacement level of RS and LD with increasing temperature is not as large as WW, which was ~ 5100–6100 for RS and ~ 5500–5900 for LD.

4. Summary of findings

Whilst there are numerous studies evaluating the different thermal techniques, most are limited to single biomass feedstocks; olive tree prunings [68], *Miscanthus giganteus* [69], straw [70,71], or mushroom compost waste [72–74]. In terms of hydrothermal conversion, the published manuscripts usually focused on only hydrothermal carbonisation as the process is mainly for hydrochar production. In this study, on the other hand, the suitability of three different biomass feedstocks (Whitewood, Rapeseed, and Seaweed (L. digitata)) was investigated for hydrochar/biochar formation, using three commonly used thermal conversion technologies; torrefaction, pyrolysis, and hydrothermal conversion (not only HTC, but also HTL and Hydrolysis). Investigation of energy application for the hydrochars produced via hydrothermal liquefaction (HTL) and/or hydrothermal hydrolysis as side product is also significantly important in order to understand the holistic approaches for full valorisation of these biomass feedstocks. This study brings several elements of novelty in that it is the first to analyse three very different feedstocks with three different thermal processing techniques, the first to compare semi-continuous hydrothermal processing to pyrolysis and torrefaction, and the first to look at optimising these processes for different feedstocks and assess the applicability of the resultant chars for bioenergy as a holistic approach. Additionally, this study is providing how useful the "**Displacement**" term is for direct comparison of these technologies regardless of feedstocks differences.

Amongst these biomass feedstocks, WW provides the greatest potential for hydrochar/biochar production across the three thermal conversion technologies used in this work, such as the hemicellulose, cellulose, and lignin structure of WW gradually decomposed with increasing temperature and also had a low ash content. During hydrothermal conversion, WW hydrochars showed a low char yield (~10–30 wt%) but a high HHV (30 kJ/g) at HTC conditions (265 °C). Additionally, biochars produced by pyrolysis at 400 °C provided a char yield (~35 wt%) with high levels of lignin and an HHV of 34 kJ/g. Similarly, biochars produced by torrefaction at intermediate temperatures (~250 °C) provided high char yields (~60 wt%) with a HHV of 25 kJ/g. Hydrochars/biochars produced by WW via hydrothermal conversion (HTC and HTL), pyrolysis (~400 °C), and torrefaction (~250 °C) could have a potential application in bioenergy production.

RS does not behave like WW with any of these thermal conversion technologies. During hydrothermal conversion, it maintains chemical composition as structure is gradually decomposed during pyrolysis. During hydrothermal conversion, RS provides slightly a higher hydrochar yield (~60 wt%) compared to WW. The hydrochars produced at the HTC conditions (235–265 °C) have a high ash content (~15 wt%) with a high HHV (~31.5 kJ/g). However, during pyrolysis, biochars produced by RS produced a reasonable biochar yield (~40 wt%) and HHV (~34 kJ/g), with an intermediate ash content (~10 wt%) and a high level of lignin at 400 °C. With torrefaction, RS produced a high biochar yield (~75 wt%), but this was, in part, due to the high levels of residual volatiles. The bioenergy application of the hydrochars/biochars produced by RS via hydrothermal conversion (HTC, HTL) and pyrolysis depends on the value of the chemicals (or biocrude) produced and any negative impact that might arise from the ash material in the chars during combustion.

LD could be used for biochemical productions through hydrothermal conversion due to its high liquefaction yield (~87 wt%) at low temperatures (200 °C). However, the hydrochars produced by LD show a low char yield (~10 wt%), low HHV (18 kJ/g), and proportionally high ash content (50 wt%) making it unsuitable for energy production. Compared with WW, it is possible to produce hydrochar from lignocellulosic biomass feedstocks (i.e. whitewood) under hydrothermal liquefaction conditions, while 90 % of seaweed was decomposed just before the defined hydrothermal carbonisation conditions (180 °C). LD does produce a high biochar yield (56–60 wt%) during pyrolysis and torrefaction at 250–300 °C. However, this char also contains high level of ash content (16–17 wt%) and low HHV (14–18 kJ/g), which makes it less desirable for energy production.

Whilst hydrothermal pressure had an insignificant effect on the structure of hydrochars produced from WW and RS, the hydrochars produced from LD under different pressure conditions show relatively different char structures i.e. a significant shift in the thermal decomposition of biopolymers was observed at the lower pressures and the peak temperature was shifted from 295 °C (240 bar) to 344 °C (55 bar). It can be concluded that hydrothermal process conditions (not only temperature but also pressure) have a significant impact on different type biomass resources.

In order to compare three thermal conversion technologies for different type of biomass feedstocks, thermal 'displacement', was used as a 'fingerprinting' technique for each biochar. The order of the highest displacement levels for these biomass feedstocks under different thermal conversion technologies were;

- WW-HC (**8181**) < WW-PC (**8900**) < WW-TC (**9400**)
- RS-HC (**3500**) < RS-TC (**6100**) < RS-PC (**7300**)
- LD-PC (**5900**) = LD-TC (**5900**) < LD-HC (**7300**)

Based on these displacement levels, the torrefaction technology appears to be the most promising technology for biochar formation from whitewood as it is shows the most significant structural 'upgrading' from its original state. Biochar produced from WW in torrefaction provides high levels of displacement (WW-TC; 9400), which demonstrate the structurally enhanced and provided a char yield (~35 wt%) with high levels of lignin and an HHV of 34 kJ/g at 280 °C. As for the RS, pyrolysis technology could be defined one of the most promising thermal conversion technologies for biochar formation from RS, where the biochar provides the highest displacement level (RS-PC; 7300) with 37 wt% of biochar yield, a strong lignin structure, and an HHV of 33.5 kJ/g at 400 °C. Although it seems a linear (direct) relation between the displacement level and quality of biochar, this is not entirely clear. Higher displacement levels are only favourable with a high biochar yield. If the biochar yield very low, a higher displacement is not a favourable situation, as observed with LD. Although the highest displacement (LD-HC; 7300) was observed with the hydrothermal conversion, the biochar yield was<10 wt% and it was predominantly ash, which is therefore not the best technology for the biochar/hydrochar production. Overall, the degree of "displacement" can help to understand and quantify the impact of process conditions of thermal conversion technologies on biochar/hydrochar formation; however, the degree of displacement should be collectively alongside other data including process yield.

5. Conclusions

This is novel research which present an extensive comparative study on how the biomass processing pathways (torrefaction, pyrolysis, and hydrothermal conversion) and process interdependencies are influenced by different feedstocks (WW, RS, and LD) for the optimisation of char (hydrochar/biochar) formation and their associated bioenergy applications. Based on the comparative evaluation of char structures, hydrochars/biochars produced by WW via hydrothermal conversion (HTC and HTL), pyrolysis (~400 °C), and torrefaction (~250 °C) could have a potential application in bioenergy production. The bioenergy application of the hydrochars/biochars produced by RS via pyrolysis depends on the value of the chemicals (or bio-oils) produced and any negative impact that might arise from the ash material in the chars during combustion. The bioenergy application of the hydrochars/biochars produced by LD via hydrothermal conversion, pyrolysis, and torrefaction is limited by the high level of ash contents and low HHV values. This study provides a clear understanding on how the thermal conversion technologies and process interdependencies influence the biochar/hydrochar formation from different type of biomass feedstocks and their potential application into the bioenergy production. As future work, combustion characteristics of the most promising biochars/hydrochars can be experimentally performed via Drop Tube Furnace (DTF) to understand the maximum capacity of these biochars in bioenergy applications. Additionally, identification of the liquid products from hydrothermal conversion and pyrolysis will provide the optimal holistic biomass processing approaches for each type of biomass feedstocks.

CRediT authorship contribution statement

Fatih Güleç: Conceptualization, Formal analysis, Investigation, Validation, Visualization, Writing – original draft, Writing – review & editing. **Orla Williams:** Conceptualization, Funding acquisition, Methodology, Supervision, Writing – review & editing. **Emily T. Kostas:** Methodology, Funding acquisition, Writing – review & editing. **Abby Samson:** Methodology, Funding acquisition, Writing – review & editing. **Edward Lester:** Conceptualization, Methodology, Supervision, Project administration, Funding acquisition, Writing – review & editing.

Declaration of Competing Interest

The authors declare that they have no known competing financial interests or personal relationships that could have appeared to influence the work reported in this paper.

Data availability

No data was used for the research described in the article.

Acknowledgements

This research was funded and supported by the EPSRC, BBSRC and UK Supergen Bioenergy Hub [Grant number EP/S000771/1], the University of Nottingham Anne McLaren Research Fellowship (Dr Orla Williams), and the UK Biotechnology and Biological Sciences Research Council (BBSRC) Discovery Fellowship (Dr Emily Kostas) [Grant number BB/S010610/1]. We also would like to acknowledge Dr David Gray, Dr Filippo Bramante, and Dr Vincenzo Di Bari for supplying the Rapeseed for this project.

Appendix A. Supplementary material

Supplementary data to this article can be found online at https://doi.org/10.1016/j.enconman.2022.116260.

References

[1] Tekin K, Karagöz S, Bektaş S. A review of hydrothermal biomass processing. Renew Sustain Energy Rev 2014;40:673–87.
[2] Shrivastava P, Khongphakdi P, Palamanit A, Kumar A, Tekasakul P. Investigation of physicochemical properties of oil palm biomass for evaluating potential of biofuels production via pyrolysis processes. Biomass Convers Biorefin 2021;11(5):1987–2001.
[3] Güleç F, Pekaslan D, Williams O, Lester E. Predictability of higher heating value of biomass feedstocks via proximate and ultimate analyses–A comprehensive study of artificial neural network applications. Fuel 2022;320:123944.

[4] Kumar M, Oyedun AO, Kumar A. A review on the current status of various hydrothermal technologies on biomass feedstock. Renew Sustain Energy Rev 2018;81:1742–70.
[5] Kostas ET, Williams OS, Duran-Jimenez G, Tapper AJ, Cooper M, Meehan R, et al. Microwave pyrolysis of Laminaria digitata to produce unique seaweed-derived bio-oils. Biomass Bioenergy 2019;125:41–9.
[6] Andersen SP, Allen B, Domingo GC. Biomass in the EU Green Deal: Towards consensus on the use of biomass for EU bioenergy. Institute for European Environmental. Policy (IEEP)2021..
[7] Şimşek EH, Güleç F, Akçadağ FS. Understanding the liquefaction mechanism of Beypazarı lignite in tetralin with ultraviolet irradiation using discrete time models. Fuel Process Technol 2020;198:106227.
[8] Şimşek EH, Güleç F, Kavuştu H, Karaduman A. Determination of liquefaction mechanisms of Zonguldak, Soma and Beypazarı coals using discrete time models. Journal of the Faculty of Engineering and Architecture of Gazi University 2019;34:79–88.
[9] Şimşek EH, Güleç F, Kavuştu H. Application of Kalman filter to determination of coal liquefaction mechanisms using discrete time models. Fuel 2017;207:814–20.
[10] E. Comission. Bioeconomy: The European Way to Use Our Natural Resources. Action Plan 2018. Office of the European Union Brussels, Belgium2018.
[11] Gunes B. A critical review on biofilm-based reactor systems for enhanced syngas fermentation processes. Renew Sustain Energy Rev 2021;143:110950.
[12] Zamri M, Hasmady S, Akhiar A, Ideris F, Shamsuddin A, Mofijur M, et al. A comprehensive review on anaerobic digestion of organic fraction of municipal solid waste. Renew Sustain Energy Rev 2021;137:110637.
[13] Arauzo PJ, Atienza-Martínez M, Ábrego J, Olszewski MP, Cao Z, Kruse A. Combustion characteristics of hydrochar and pyrochar derived from digested sewage sludge. Energies 2020;13:4164.
[14] Fan F, Xing X, Shi S, Zhang X, Zhang X, Li Y, et al. Combustion characteristic and kinetics analysis of hydrochars. Transactions of the Chinese Society of Agricultural Engineering 2016;32:219–24.
[15] Kostas ET, Durán-Jiménez G, Shepherd BJ, Meredith W, Stevens LA, Williams OS, et al. Microwave pyrolysis of olive pomace for bio-oil and bio-char production. Chem Eng J 2020;387:123404.
[16] Wang S, Dai G, Yang H, Luo Z. Lignocellulosic biomass pyrolysis mechanism: a state-of-the-art review. Prog Energy Combust Sci 2017;62:33–86.
[17] Yang H, Yan R, Chen H, Lee DH, Zheng C. Characteristics of hemicellulose, cellulose and lignin pyrolysis. Fuel 2007;86:1781–8.
[18] Abdoulmoumine N, Adhikari S, Kulkarni A, Chattanathan S. A review on biomass gasification syngas cleanup. Appl Energy 2015;155:294–307.
[19] Cao L, Iris K, Xiong X, Tsang DC, Zhang S, Clark JH, et al. Biorenewable hydrogen production through biomass gasification: A review and future prospects. Environ Res 2020;186:109547.
[20] Güleç F, Riesco LMG, Williams O, Kostas ET, Samson A, Lester E. Hydrothermal conversion of different lignocellulosic biomass feedstocks–Effect of the process conditions on hydrochar structures. Fuel 2021;302:121166.
[21] Shen Y. A review on hydrothermal carbonization of biomass and plastic wastes to energy products. Biomass Bioenergy 2020;134:105479.
[22] Antero RVP, Alves ACF, de Oliveira SB, Ojala SA, Brum SS. Challenges and alternatives for the adequacy of hydrothermal carbonization of lignocellulosic biomass in cleaner production systems: A review. J Cleaner Prod 2020;252:119899.
[23] Wilk M, Magdziarz A, Jayaraman K, Szymańska-Chargot M, Gökalp I. Hydrothermal carbonization characteristics of sewage sludge and lignocellulosic biomass. A comparative study Biomass and Bioenergy 2019;120:166–75.
[24] Sharma R, Jasrotia K, Singh N, Ghosh P, srivastava S, Sharma NR, et al. A Comprehensive Review on Hydrothermal Carbonization of Biomass and its Applications. Chemistry. Africa 2019;3:1–19.
[25] Güleç F, Samson A, Williams O, Kostas ET, Lester E. Biofuel characteristics of chars produced from rapeseed, whitewood, and seaweed via thermal conversion technologies – Impacts of feedstocks and process conditions. Fuel Process Technol 2022;238:107492.
[26] Lan K, Park S, Yao Y. Key issue, challenges, and status quo of models for biofuel supply chain design. In: Biofuels for a more sustainable future; 2020. p. 273–315.
[27] Manahan SE. Environmental science and technology: a sustainable approach to green science and technology. CRC Press; 2006.
[28] Güleç F, Özdemir GDT. Investigation of drying characteristics of Cherry Laurel (Laurocerasus officinalis Roemer) fruits. Akademik ziraat dergisi 2017;6:73–80.
[29] Ong HC, Chen W-H, Singh Y, Gan YY, Chen C-Y, Show PL. A state-of-the-art review on thermochemical conversion of biomass for biofuel production: A TG-FTIR approach. Energy Convers Manage 2020;209:112634.
[30] Alper K, Tekin K, Karagöz S, Ragauskas AJ. Sustainable energy and fuels from biomass: a review focusing on hydrothermal biomass processing. Sustainable Energy Fuels 2020;4(9):4390–414.
[31] Alves O, Nobre C, Durão L, Monteiro E, Brito P, Gonçalves M. Effects of dry and hydrothermal carbonisation on the properties of solid recovered fuels from construction and municipal solid wastes. Energy Convers Manage 2021;237:114101.
[32] Li Q, Faramarzi A, Zhang S, Wang Y, Hu X, Gholizadeh M. Progress in catalytic pyrolysis of municipal solid waste. Energy Convers Manage 2020;226:113525.
[33] Lee XJ, Ong HC, Gan YY, Chen W-H, Mahlia TMI. State of art review on conventional and advanced pyrolysis of macroalgae and microalgae for biochar, bio-oil and bio-syngas production. Energy Convers Manage 2020;210:112707.
[34] Scarlat N, Dallemand J, Taylor N, Banja M, Sanchez Lopez J, Avraamides M. Brief on biomass for energy in the European Union. Luxembourg: Publications Office of the European Union; 2019.
[35] Güleç F, Williams O, Kostas ET, Samson A, Stevens LA, Lester E. A comprehensive comparative study on methylene blue removal from aqueous solution using biochars produced from rapeseed, whitewood, and seaweed via different thermal conversion technologies. Fuel 2022;330:125428.
[36] Isikgor FH, Becer CR. Lignocellulosic biomass: a sustainable platform for the production of bio-based chemicals and polymers. Polym Chem 2015;6:4497–559.
[37] Guo M, Song W. The growing US bioeconomy: Drivers, development and constraints. New Biotechnol 2019;49:48–57.
[38] Güleç F, Şimşek EH, Sarı HT. Prediction of biomass pyrolysis mechanisms and kinetics–Application of Kalman filter. Chem Eng Technol 2022;45:167–77.
[39] Williams O, Newbolt G, Eastwick C, Kingman S, Giddings D, Lormor S, et al. Influence of mill type on densified biomass comminution. Appl Energy 2016;182:219–31.
[40] Williams O, Eastwick C, Kingman S, Giddings D, Lormor S, Lester E. Investigation into the applicability of Bond Work Index (BWI) and Hardgrove Grindability Index (HGI) tests for several biomasses compared to Colombian La Loma coal. Fuel 2015;158:379–87.
[41] Vassilev SV, Vassileva CG, Vassilev VS. Advantages and disadvantages of composition and properties of biomass in comparison with coal: An overview. Fuel 2015;158:330–50.
[42] Okolie JA, Epelle EI, Tabat ME, Orivri U, Amenaghawon AN, Okoye PU, et al. Waste biomass valorization for the production of biofuels and value-added products: A comprehensive review of thermochemical, biological and integrated processes. Process Saf Environ Prot 2022;159:323–44.
[43] Jha S, Okolie JA, Nanda S, Dalai AK. A review of biomass resources and thermochemical conversion technologies. Chem Eng Technol 2022;45:791–9.
[44] Pandey D, Daverey A, Arunachalam K. Biochar: Production, properties and emerging role as a support for enzyme immobilization. J Cleaner Prod 2020;255:120267.
[45] Nhuchhen DR, Basu P, Acharya B. A comprehensive review on biomass torrefaction. International Journal of Renewable Energy & Biofuels 2014;2014:1–56.
[46] Pohlmann JG, Osório E, Vilela AC, Diez MA, Borrego AG. Integrating physicochemical information to follow the transformations of biomass upon torrefaction and low-temperature carbonization. Fuel 2014;131:17–27.
[47] Thengane SK, Kung K, York R, Sokhansanj S, Lim CJ, Sanchez DL. Technoeconomic and emissions evaluation of mobile in-woods biochar production. Energy Convers Manage 2020;223:113305.
[48] Hao W, Björkman E, Lilliestråle M, Hedin N. Activated carbons for water treatment prepared by phosphoric acid activation of hydrothermally treated beer waste. Ind Eng Chem Res 2014;53:15389–97.
[49] Subedi R, Kammann C, Pelisseti S, Sacco D, Grignani C, Monaco S. Recycling of organic residues for agriculture: from waste management to ecosystem services. 15th International Conference RAMIRAN 2013.
[50] Guangzhi Y, Jinyu Y, Yuhua Y, Zhihong T, DengGuang Y, Junhe Y. Preparation and CO 2 adsorption properties of porous carbon from camphor leaves by hydrothermal carbonization and sequential potassium hydroxide activation. RSC Adv 2017;7:4152–60.
[51] Liu Z, Zhang F, Hoekman SK, Liu T, Gai C, Peng N. Homogeneously dispersed zerovalent iron nanoparticles supported on hydrochar-derived porous carbon: simple, in situ synthesis and use for dechlorination of PCBs. ACS Sustainable Chem Eng 2016;4:3261–7.
[52] Titirici M-M, Antonietti M, Baccile N. Hydrothermal carbon from biomass: a comparison of the local structure from poly-to monosaccharides and pentoses/hexoses. Green Chem 2008;10:1204–12.
[53] Lester E, Avila C, Pang CH, Williams O, Perkins J, Gaddipatti S, et al. A proposed biomass char classification system. Fuel 2018;232:845–54.
[54] Chen W-H, Lin B-J, Lin Y-Y, Chu Y-S, Ubando AT, Show PL, et al. Progress in biomass torrefaction: Principles, applications and challenges. Prog Energy Combust Sci 2021;82:100887.
[55] Mamvura TA, Danha G. Biomass torrefaction as an emerging technology to aid in energy production. Heliyon 2020;6:e03531.
[56] Isemin R, Mikhalev A, Milovanov O, Klimov D, Kokh-Tatarenko V, Brulé M, et al. Comparison of Characteristics of Poultry Litter Pellets Obtained by the Processes of Dry and Wet Torrefaction. Energies 2022;15:2153.
[57] Zhang Q, Chang J, Wang T, Xu Y. Review of biomass pyrolysis oil properties and upgrading research. Energy Convers Manage 2007;48:87–92.
[58] Hameed S, Sharma A, Pareek V, Wu H, Yu Y. A review on biomass pyrolysis models: Kinetic, network and mechanistic models. Biomass Bioenergy 2019;123:104–22.
[59] Khuenkaeo N, Phromphithak S, Onsree T, Naqvi SR, Tippayawong N. Production and characterization of bio-oils from fast pyrolysis of tobacco processing wastes in an ablative reactor under vacuum. PLoS ONE 2021;16:e0254485.
[60] Basu P. Biomass gasification, pyrolysis and torrefaction: practical design and theory. Academic press; 2018.
[61] Ruiz HA, Rodríguez-Jasso RM, Fernandes BD, Vicente AA, Teixeira JA. Hydrothermal processing, as an alternative for upgrading agriculture residues and marine biomass according to the biorefinery concept: a review. Renew Sustain Energy Rev 2013;21:35–51.
[62] Pedersen TH, Grigoras I, Hoffmann J, Toor SS, Daraban IM, Jensen CU, et al. Continuous hydrothermal co-liquefaction of aspen wood and glycerol with water phase recirculation. Appl Energy 2016;162:1034–41.
[63] Heidari M, Dutta A, Acharya B, Mahmud S. A review of the current knowledge and challenges of hydrothermal carbonization for biomass conversion. J Energy Inst 2019;92:1779–99.

[64] Cheng C, Ding L, Guo Q, He Q, Gong Y, Alexander KN, et al. Process analysis and kinetic modeling of coconut shell hydrothermal carbonization. Appl Energy 2022; 315:118981.
[65] Liu T, Jiao H, Yang L, Zhang W, Hu Y, Guo Y, et al. Co-hydrothermal carbonization of cellulose, hemicellulose, and protein with aqueous phase recirculation: Insight into the reaction mechanisms on hydrochar formation. Energy 2022;251:123965.
[66] Leng L, Yang L, Chen J, Hu Y, Li H, Li H, et al. Valorization of the aqueous phase produced from wet and dry thermochemical processing biomass: A review. J Cleaner Prod 2021;294:126238.
[67] Cheng C, He Q, Ismail TM, Mosqueda A, Ding L, Yu J, et al. Hydrothermal carbonization of rape straw: Effect of reaction parameters on hydrochar and migration of AAEMs. Chemosphere 2022;291:132785.
[68] González-Arias J, Gómez X, González-Castaño M, Sanchez ME, Rosas JG, Cara-Jiménez J. Insights into the product quality and energy requirements for solid biofuel production: A comparison of hydrothermal carbonization, pyrolysis and torrefaction of olive tree pruning. Energy 2022;238:122022.
[69] Wilk M, Magdziarz A. Hydrothermal carbonization, torrefaction and slow pyrolysis of Miscanthus giganteus. Energy 2017;140:1292–304.
[70] Chen L, Wen C, Wang W, Liu T, Liu E, Liu H, et al. Combustion behaviour of biochars thermally pretreated via torrefaction, slow pyrolysis, or hydrothermal carbonisation and co-fired with pulverised coal. Renewable Energy 2020;161: 867–77.
[71] Wang W, Wen C, Li C, Wang M, Li X, Zhou Y, et al. Emission reduction of particulate matter from the combustion of biochar via thermal pre-treatment of torrefaction, slow pyrolysis or hydrothermal carbonisation and its co-combustion with pulverized coal. Fuel 2019;240:278–88.
[72] Atallah E, Zeaiter J, Ahmad MN, Leahy JJ, Kwapinski W. Hydrothermal carbonization of spent mushroom compost waste compared against torrefaction and pyrolysis. Fuel Process Technol 2021;216:106795.
[73] Wang Y, Qiu L, Zhu M, Sun G, Zhang T, Kang K. Comparative evaluation of hydrothermal carbonization and low temperature pyrolysis of eucommia ulmoides oliver for the production of solid biofuel. Sci Rep 2019;9:1–11.
[74] Miliotti E, Casini D, Rosi L, Lotti G, Rizzo AM, Chiaramonti D. Lab-scale pyrolysis and hydrothermal carbonization of biomass digestate: Characterization of solid products and compliance with biochar standards. Biomass Bioenergy 2020;139: 105593.
[75] Correa CR, Hehr T, Voglhuber-Slavinsky A, Rauscher Y, Kruse A. Pyrolysis vs. hydrothermal carbonization: Understanding the effect of biomass structural components and inorganic compounds on the char properties. J Anal Appl Pyrol 2019;140:137–47.
[76] Babinszki B, Jakab E, Sebestyén Z, Blazsó M, Berényi B, Kumar J, et al. Comparison of hydrothermal carbonization and torrefaction of azolla biomass: Analysis of the solid products. J Anal Appl Pyrol 2020;149:104844.
[77] Pala M, Kantarli IC, Buyukisik HB, Yanik J. Hydrothermal carbonization and torrefaction of grape pomace: A comparative evaluation. Bioresour Technol 2014; 161:255–62.
[78] Kambo HS, Dutta A. Comparative evaluation of torrefaction and hydrothermal carbonization of lignocellulosic biomass for the production of solid biofuel. Energy Convers Manage 2015;105:746–55.
[79] Duman G, Balmuk G, Cay H, Kantarli IC, Yanik J. Comparative evaluation of torrefaction and hydrothermal carbonization: Effect on fuel properties and combustion behavior of agricultural wastes. Energy Fuels 2020;34:11175–85.
[80] Lokmit C, Nakason K, Kuboon S, Jiratanachotikul A, Panyapinyopol B. Enhancing lignocellulosic energetic properties through torrefaction and hydrothermal carbonization processes. Biomass Convers Biorefin 2022:1–13.
[81] Lampropoulos A, Kaklidis N, Athanasiou C, Montes-Morán MA, Arenillas A, Menéndez JA, et al. Effect of Olive Kernel thermal treatment (torrefaction vs. slow pyrolysis) on the physicochemical characteristics and the CO2 or H2O gasification performance of as-prepared biochars. Int J Hydrogen Energy 2021; 46:29126–41.
[82] Prashanth PF, Gurrala L, Mohan RV, Sarvanakumar K, Vinu R. Microwave-assisted torrefaction and pyrolysis of rice straw pellets for bioenergy. IET Renew Power Gener 2022.
[83] Azwar E, Mahari WAW, Rastegari H, Tabatabaei M, Peng W, Tsang YF, et al. Progress in thermochemical conversion of aquatic weeds in shellfish aquaculture for biofuel generation: Technical and economic perspectives. Bioresour Technol 2022;344:126202.
[84] Heikkinen J, Keskinen R, Soinne H, Hyväluoma J, Nikama J, Wikberg H, et al. Possibilities to improve soil aggregate stability using biochars derived from various biomasses through slow pyrolysis, hydrothermal carbonization, or torrefaction. Geoderma 2019;344:40–9.
[85] Lester E, Gong M, Thompson A. A method for source apportionment in biomass/coal blends using thermogravimetric analysis. J Anal Appl Pyrol 2007;80:111–7.
[86] Kostas ET, White DA, Cook DJ. Development of a bio-refinery process for the production of speciality chemical, biofuel and bioactive compounds from Laminaria digitata. Algal research 2017;28:211–9.
[87] De Chirico S, di Bari V, Guzmán MJR, Nikiforidis CV, Foster T, Gray D. Assessment of rapeseed oil body (oleosome) lipolytic activity as an effective predictor of emulsion purity and stability. Food Chem 2020;316:126355.
[88] De Chirico S, di Bari V, Foster T, Gray D. Enhancing the recovery of oilseed rape seed oil bodies (oleosomes) using bicarbonate-based soaking and grinding media. Food Chem 2018;241:419–26.
[89] Paczkowski S, Sauer C, Anetzberger A, Paczkowska M, Russ M, Wöhler M, et al. Feedstock particle size distribution and water content dynamic in a pellet mill production process and comparative sieving performance of horizontal 3.15-mm mesh and 3.15-mm hole sieves. Biomass Convers Biorefin 2019:1–12.
[90] EN-ISO-17827-2. Solid biofuels - determination of particle size distribution for uncompressed fuels: Part 2: Vibrating screen method using sieves with aperture of 3,15 mm and below (17827-2:2016-10). DIN Deutsches Insitut für Normung2016.
[91] Adams J, Ross A, Anastasakis K, Hodgson E, Gallagher J, Jones J, et al. Seasonal variation in the chemical composition of the bioenergy feedstock Laminaria digitata for thermochemical conversion. Bioresour Technol 2011;102:226–34.
[92] Güleç F, Meredith W, Sun C-G, Snape CE. Demonstrating the applicability of chemical looping combustion for the regeneration of fluid catalytic cracking catalysts. Chem Eng J 2020;389:124492.
[93] Güleç F. Demonstrating the applicability of chemical looping combustion for fluid catalytic cracking unit as a novel CO2 capture technology. Chemical Engineering. University of Nottingham 2020.
[94] Yin C-Y. Prediction of higher heating values of biomass from proximate and ultimate analyses. Fuel 2011;90:1128–32.
[95] Callejón-Ferre A, Velázquez-Martí B, López-Martínez J, Manzano-Agugliaro F. Greenhouse crop residues: Energy potential and models for the prediction of their higher heating value. Renew Sustain Energy Rev 2011;15:948–55.
[96] Tillman DA. Wood as an energy resource. Elsevier; 2012.
[97] Güleç F, Erdogan A, Clough PT, Lester E. Investigation of the hydrodynamics in the regenerator of fluid catalytic cracking unit integrated by chemical looping combustion. Fuel Process Technol 2021;223:106998.
[98] Güleç F, Meredith W, Sun C-G, Snape CE. A novel approach to CO2 capture in fluid catalytic cracking—chemical looping combustion. Fuel 2019;244:140–50.
[99] Güleç F, Meredith W, Sun C-G, Snape CE. Selective low temperature chemical looping combustion of higher alkanes with Cu-and Mn-oxides. Energy 2019;173: 658–66.
[100] Koechermann J, Goersch K, Wirth B, Muehlenberg J, Klemm M. Hydrothermal carbonization: Temperature influence on hydrochar and aqueous phase composition during process water recirculation. J Environ Chem Eng 2018;6: 5481–7.
[101] Ninduangdee P, Kuprianov VI, Cha EY, Kaewrath R, Youngyuen P, Atthawethworawuth W. Thermogravimetric studies of oil palm empty fruit bunch and palm kernel shell: TG/DTG analysis and modeling. Energy Procedia 2015;79: 453–8.
[102] Kostas ET, White DA, Du C, Cook DJ. Selection of yeast strains for bioethanol production from UK seaweeds. J Appl Phycol 2016;28:1427–41.
[103] Chandra S, Bhattacharya J. Influence of temperature and duration of pyrolysis on the property heterogeneity of rice straw biochar and optimization of pyrolysis conditions for its application in soils. J Cleaner Prod 2019;215:1123–39.
[104] Zhao S-X, Ta N, Wang X-D. Effect of temperature on the structural and physicochemical properties of biochar with apple tree branches as feedstock material. Energies 2017;10:1293.
[105] Elliott DC, Biller P, Ross AB, Schmidt AJ, Jones SB. Hydrothermal liquefaction of biomass: developments from batch to continuous process. Bioresour Technol 2015;178:147–56.
[106] Arellanoa O, Flores M, Guerra J, Hidalgo A, Rojas D, Strubinger A. Hydrothermal carbonization (HTC) of corncob and characterization of the obtained hydrochar. Chem Eng 2016;50.
[107] Carrier M, Auret L, Bridgwater A, Knoetze JH. Using apparent activation energy as a reactivity criterion for biomass pyrolysis. Energy Fuels 2016;30:7834–41.
[108] Maryandyshev P, Chernov A, Popova E, Eseev M, Lyubov V. The isothermal degradation of wood. Solid Fuel Chem 2016;50:381–9.
[109] Ucar S, Ozkan AR. Characterization of products from the pyrolysis of rapeseed oil cake. Bioresour Technol 2008;99:8771–6.
[110] Smets K, Roukaerts A, Czech J, Reggers G, Schreurs S, Carleer R, et al. Slow catalytic pyrolysis of rapeseed cake: Product yield and characterization of the pyrolysis liquid. Biomass Bioenergy 2013;57:180–90.
[111] Dahl L. Composition of Laminaria digitata biomass during a potential. 2018.
[112] He Q, Raheem A, Ding L, Xu J, Cheng C, Yu G. Combining wet torrefaction and pyrolysis for woody biochar upgradation and structural modification. Energy Convers Manage 2021;243:114383.
[113] Chen W-H, Eng CF, Lin Y-Y, Bach Q-V, Ashokkumar V, Show P-L. Two-step thermodegradation kinetics of cellulose, hemicelluloses, and lignin under isothermal torrefaction analyzed by particle swarm optimization. Energy Convers Manage 2021;238:114116.
[114] Gan YY, Chen W-H, Ong HC, Lin Y-Y, Sheen H-K, Chang J-S, et al. Effect of wet torrefaction on pyrolysis kinetics and conversion of microalgae carbohydrates, proteins, and lipids. Energy Convers Manage 2021;227:113609.
[115] Weiss IM, Muth C, Drumm R, Kirchner HO. Thermal decomposition of the amino acids glycine, cysteine, aspartic acid, asparagine, glutamic acid, glutamine, arginine and histidine. BMC biophysics 2018;11:1–15.
[116] Membere E, Sallis P. Thermochemical characterization of brown seaweed, Laminaria digitata from UK shores. J Anal Appl Pyrol 2018;131:42–51.
[117] Palanisamy S, Gevert BS. Study of non-catalytic thermal decomposition of triglyceride at hydroprocessing condition. Appl Therm Eng 2016;107:301–10.
[118] Ericson M, Rödin J, Lenman M, Glimelius K, Josefsson L-G, Rask L. Structure of the rapeseed 1.7 S storage protein, napin, and its precursor. J Biol Chem 1986; 261:14576–81.